Environmental Science and Pollution Research (2023) 30:11959–11977
https://doi.org/10.1007/s11356-022-22967-0

RESEARCH ARTICLE

The efficient degradation of diclofenac by ferrate and peroxymonosulfate: performances, mechanisms, and toxicity assessment

Haonan He[1] · Junfeng Zhao[1,2,3]

Received: 4 May 2022 / Accepted: 5 September 2022 / Published online: 14 September 2022

Abstract

In this study, the degradation efficiency and reaction mechanisms of diclofenac (DCF), a nonsteroidal anti-inflammatory drug, by the combination of ferrate (Fe(VI) and peroxymonosulfate (PMS) (Fe(VI)/PMS) were systematically investigated. The higher degradation efficiency of DCF in Fe(VI)/PMS system can be obtained than that in alone persulfate (PS), Fe(VI), PMS, or the Fe(VI)/PS process at pH 6.0. DCF was efficiently removed in Fe(VI)/PMS process within a wide range of pH values from 4.0 to 8.0, with higher degradation efficiency in acidic conditions. The increasing reaction temperature (10 to 30 ℃), Fe(VI) dose (6.25 to 100 μM), or PMS concentration (50 to 1000 μM) significantly enhanced the DCF degradation. The existences of HCO_3^-, Cl^-, and humic acid (HA) obviously inhibited the DCF removal. Electron paramagnetic resonance (EPR), free radical quenching, and probing experiments confirmed the existence of sulfate radicals ($SO_4^{\bullet-}$), hydroxyl radicals ($^{\bullet}OH$), and Fe(V)/ Fe(IV), which are responsible for DCF degradation in Fe(VI)/PMS system. The variations of TOC removal ratio reveal that the adsorption of organics with ferric particles, formed in the reduction of Fe(VI), also were functioned in the removal process. Sixteen DCF transformation byproducts were identified by UPLC-QTOF/MS, and the toxicity variation was evaluated. Consequently, eight reaction pathways for DCF degradation were proposed. This study provides theoretical basis for the utilization of Fe(VI)/PMS process.

Keywords Ferrate · Peroxymonosulfate · Diclofenac · Reaction pathways · Toxicity assessment

Responsible Editor: Ricardo A. Torres-Palma

Highlights

- Fe(VI), Fe(V), Fe(IV), $SO4^{\bullet-}$ and $^{\bullet}OH$ were responsible for the degradation of DCF.
- Fe(VI)/PMS process could efficiently degrade DCF with pH range from 4.0 to 8.0.
- Eight transformation pathways were proposed based on the identified by-products.
- High removal efficiency of DCF was obtained in different real waters by Fe(VI)/PMS.

✉ Junfeng Zhao
zhaojunfeng1314@163.com

[1] College of Chemistry and Materials Science, Sichuan Normal University, Jingan Road 5#, Jinjiang District, Chengdu 610066, Sichuan, China

[2] Key Laboratory of Special Waste Water Treatment, Sichuan Province Higher Education System, Sichuan, Chengdu 610066, China

[3] Key Laboratory of Land Resources Evaluation and Monitoring in Southwest, Ministry of Education of China, Chengdu 610066, China

Introduction

Diclofenac (DCF) belongs to the family of nonsteroidal anti-inflammatory drugs (NSAIDs). And its sodium salt (diclofenac sodium) is widely used for treating painful inflammatory rheumatoid and non-rheumatoid diseases, acting as an analgesic, antipyretic, anti-arthritic, and anti-rheumatic drug (Oral and Kantar 2019; Wang et al. 2021). The structure and physico-chemical properties of DCF are shown in Fig. 1 and Table S1 in the "Supplementary information" (SI). As an "emerging contaminant" (EC), DCF is difficult to biodegrade, and its removal in conventional wastewater treatment plants (WWTPs) is limited and incomplete (20–40%) (Joss et al. 2005). The existences of DCF in WWTP effluents, surface water, ground water, and even drinking water have been detected (ng L^{-1} to μg L^{-1}) (Huguet et al. 2013; Bu et al. 2013). Therefore, DCF is easily discharged into the aqueous environment, which may have unpredictable impact on the ecological system and human health although with low concentration (Petrie et al. 2015).

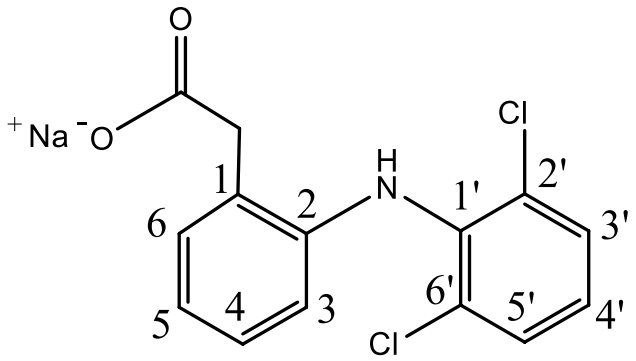

Fig. 1 Structure of DCF

It is urgent to develop economic, effective, and environmentally friendly treatment technologies for DCF destruction in aquatic environment.`

In recent years, DCF degradation by various advanced oxidation processes (AOPs) have been studied due to the strong oxidation capability of various free radicals, such as hydroxyl radicals, sulfate radicals, and singlet oxygen (Wang and Bai 2017; Wang and Wang 2018; Huang et al. 2020; Xu et al. 2022). With the wide pH range (2–8), high redox potential (2.5–3.1 V), long half-life (30–40 μs), and selective oxidation ability, sulfate radical ($SO_4^{\bullet-}$)–based AOPs have gained intensive interest and been extensively used in the removal of ECs in water (Olmez-Hanci and Arslan-Alaton 2013; Sharma et al. 2015a; Berruti et al. 2022). Peroxymonosulfate (PMS, HSO_5^-) can be applied to produce $SO_4^{\bullet-}$ but with extremely sluggish formation rate, which makes the direct use of PMS become impractical. Various approaches for activating PMS to $SO_4^{\bullet-}$ have been studied, such as heat, microwave, ultrasound, ultraviolet light, and transition metals (Khan et al. 2014; Oh et al. 2016; Ghanbari and Moradi 2017; Gao et al. 2022; Zhao et al. 2022a). Despite the rapid generation of $SO_4^{\bullet-}$, the significant drawbacks of these activating approaches cannot be ignored. On one hand, the energy activation–based processes for PMS (heat, UV radiation, etc.) require continuous energy input, which are uneconomical and complicated. On the other hand, the homogeneous or heterogeneous transition metal activation–based systems may result the leaching of toxic metal ions and cause health concerns due to its potential toxicity (such as Co^{3+}) (Simonsen et al. 2012; Zhao et al. 2022b). Of the various approaches to activate PMS, iron-based activators, such as Fe^{3+}, Fe^{2+}, and nanoscale zerovalent iron (Fe^0), have advantages due to their greener and sustainable properties (Xiao et al. 2020). However, the practical application of these activators are restricted owing to the rapid consumption of $SO_4^{\bullet-}$ by excess Fe^{2+} and the slow conversion from Fe^{3+} to Fe^{2+} (Li et al. 2020).

Ferrate (Fe(VI)), an emerging green oxidant, coagulant, and disinfectant, presents a high redox potential from + 2.20 V to + 0.72 V in acidic and basic solutions, respectively (Sharma 2008). Fe(VI) can effectively eliminate various refractory contaminants, such as endocrine-disrupting chemicals (EDCs) (Yang et al. 2012; Wang et al. 2022), pharmaceuticals and personal care products (PPCPs) (Sun et al. 2019), heavy metal ions (As(III), Sb(III), etc.) (Lan et al. 2016), and bacteria and viruses (Manoli et al. 2020). Previous studies have revealed that Fe(VI) preferentially oxidized organic contaminants with electron-rich moieties via electron-transfer and oxygen-transfer mechanisms (Lee et al. 2005; Shi et al. 2022). In addition, during the Fe(VI) oxidation, the formation of undesirable disinfection byproducts can be avoided (Jiang et al. 2016), and the transformation products of Fe(VI), such as Fe^{3+} and Fe^{2+}, can be used as coagulants to promote the removal of contaminants (Jiang 2014; Yu et al. 2022). Even so, the rapid self-decay of Fe(VI) is unavoidable in water (Eqs. (1) and (2)), which significantly weakens the oxidation capacity of Fe(VI) (Al-Abduly and Sharma 2014). The drawback restricted the application of Fe(VI).

$$FeO_4^{2-} + 8H^+ + 3e^- \rightarrow Fe^{3+}4H_2O \quad (1)$$

$$FeO_4^{2-} + 4H_2O + 3e^- \rightarrow Fe(OH)_3 + 50H^- \quad (2)$$

Recently, the combination of Fe(VI) and various chemicals for the enhancing oxidation of organic pollutants has been put forward as an innovative chemical oxidation technology. For example, during the degradation of enrofloxacin and phenol in Fe(VI)/sulfite process, the degradation efficiency was significantly improved, and both Fe(V), $SO_4^{\bullet-}$ and $^{\bullet}OH$ contributed to the micropollutants' removal (Shao et al. 2020; Yang et al. 2022). Wu et al. investigated the atrazine removal by Fe(VI)/PMS process with higher degradation efficiency than that of Fe(VI)/persulfate or Fe(VI)/H_2O_2 process at pH 6.0. Also, both hydroxyl radical and sulfate radical were detected in the Fe(VI)/PMS process (Wu et al. 2018b). Nevertheless, studies systematically investigated the removal efficiency and mechanism of DCF by the Fe(VI)/PMS process are still imperative.

In this study, the combined use of Fe(VI) and PMS for the continuous removal of DCF was systematically investigated. This study aimed to (i) assess the feasibility of Fe(VI)/PMS process for DCF removal; (ii) evaluate the effects of experimental conditions (e.g., initial pH, reaction temperature, dosage of Fe(VI) and PMS) and water matrix (e.g., HCO_3^-, Cl^-, NO_3^-, SO_4^{2-}, humic acid (HA)) for DCF degradation; (iii) identify the reactive species by electron paramagnetic resonance (EPR), free radical quenching, and probing experiments; (iv) explore the variations of TOC removal ratio; (v)

identify the reaction intermediates of DCF and propose the decay pathway; and (vi) evaluate the toxicity of DCF and its intermediates. The findings of this study will give a new insight on removing DCF by the Fe(VI)/PMS process.

Materials and methods

Materials

Diclofenac sodium (DCF, 99% purity), peroxymonosulfate (PMS, ≥ 47% $KHSO_5$ basis), persulfate (PS), humic acid (HA, used as natural organic matter (NOM)), 5,5-dimethyl-1-pyrroline N-oxide (DMPO, > 97.0%), methyl phenyl sulfoxide (PMSO, 98%), and methyl phenyl sulfone ($PMSO_2$) were obtained from Aladdin Chemistry Co., Ltd (Shanghai, China). Potassium ferrate (K_2FeO_4, Fe(VI), 92% purity) was prepared using the modified wet oxidation method (Delaude and Laszlo 1996) and used as solid powder in the experiment. The purity of solid Fe(VI) was measured daily by direct spectrophotometric method using an Unico-2150 UV/VIS spectrophotometer (Unico (Shanghai) Instrument Co., Ltd.) at a wavelength of 505 nm (Jiang et al. 2009). Methanol (MeOH) and acetic acid were HPLC grade, and other chemicals (e.g., *tert*-butanol (TBA), *n*-hexane, $KMnO_4$, H_2SO_4, KOH, NaOH, HCl, $Na_2S_2O_3{\cdot}5H_2O$, NaCl and Na_2CO_3) were analytic grade, which were all purchased from Sinopharm Chemical Reagent Co. Ltd. (China). All solutions were prepared using ultrapure water.

Experimental procedures

All batch experiments were conducted in 2-L beakers with a water-bath shaker (250 rpm). Typically, 1000 mL of 5 μM DCF solution was prepared, and the solution pH was adjusted by 1/15 M Na_2HPO_4, 1/15 M KH_2PO_4 and 0.2 M NaOH in advance (as shown in SI Table S2). The desired amount of PMS or PS was added to the above solution, and then a certain amount of Fe(VI) was added instantly to initiate the reaction. At defined time intervals, 3-mL samples were obtained and promptly quenched by 50 μL of 11 mM $Na_2S_2O_3$. Before analyzing the concentration of DCF by ultra-high performance liquid chromatograph (UPLC), the samples were filtered by 0.22-μm glass fiber filters (Xingya Purifying Material Factory, China), or dissolved with 0.5% of HCl. To confirm the contributions of the reactive oxidation species (ROSs), quenching experiments were carried out using MeOH and TAB as radical scavengers. In addition, five different water samples were collected, including ultra-pure water, tap water, and samples from the Yangliu River (1#), Luxi River (2 #) and Jing Lake (Chengdu, China). The samples were all filtered through 0.45-μm glass fiber filters and stored at 4 ℃. DCF solutions in different water samples were prepared at a concentration of 5 μM by magnetic stirring for 24 h.

All experiments were performed in triplicate.

Analytical methods

The DCF concentration was determined by an Agilent 1290 ultra-high performance liquid chromatograph (UPLC, Agilent, USA) with a diode array detector (DAD, setting at 276 nm) equipped with a reverse-phase Symmetry C18 analytical column (5 μm, 4.6 × 150 mm, Agilent, USA). The column temperature was kept at 30 °C and the injection volume was 20 μL. The mobile phase was composed of 75% methanol and 25% ultrapure water (containing 1‰ acetic acid) at a flow rate of 0.3 mL min^{-1}.

The intermediate products of DCF were identified by a SCIEX ultraperformance liquid chromatograph coupled with a SCIEX X500R quadrupole-time of flight-mass spectrometer (UPLC- QTOF/MS). The mobile phase consisted of A (acetonitrile) and B (1‰ acetic acid in ultrapure water), and the gradient elution was as follows: 0–2 min 1% A and 99% B, 2–3 min a linear gradient to 20% A and 80% B, 3–20 min 20% A and 80% B, 20–33 min a linear gradient to 99% A and 1% B, 33–42 min 99% A and 1% B, and 42–43 min a linear gradient to 1% A and 99% B. The injection volume was 10 μL for each sample and the flow rate was set at 1 mL min^{-1}. The mass spectra was conducted with negative electrospray ionization (ESI^-) with the scan scope of *m/z* 50–500.

Total organic carbon (TOC) concentration was determined by Multi N/C 3000 TOC analyzer (Analytik Jena AG, Germany). Electron paramagnetic resonance (EPR) spectra of free radicals were measured on a Bruker EMX nanospectrometer (Bruker, Germany) using 5,5-dimethyl-1-pyrroline N-oxide (DMPO) as spin-strapping agent. The concentrations of PMSO and $PMSO_2$ were analyzed with liquid chromatography (Huang et al. 2021). The concentrations of Fe(II) and Fe(III) in solution were detected at 510 nm by the 1,10-phenanthroline method with a Unico-2150 UV/VIS spectrophotometer (Unico (Shanghai) Instrument Co., Ltd.). PMS concentration was measured by a modified iodide spectrophotometry method (Liang et al. 2008). The solution pH was measured by a portable pH meter ($pHS\text{-}4C^+$, China).

Toxicity measurements

The Ecological Structure–Activity Relationship (ECOSAR) software was utilized to predict the acute toxicity (LC_{50} or EC_{50}) and chronic toxicity (ChV) of DCF and its intermediates to three aquatic organisms (fish, daphnid, and green algae) during the Fe(VI)/PMS process (Yang et al. 2019).

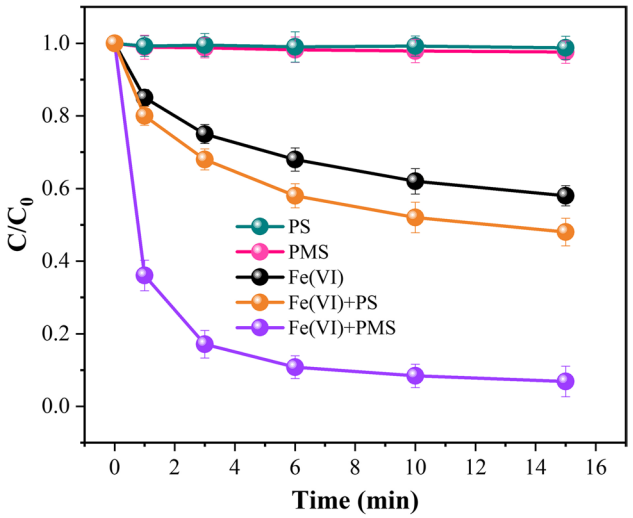

Fig. 2 Degradation of DCF by various oxidants. Experimental conditions: $[PS]_0 = [PMS]_0 = 500$ μM, $[Fe(VI)]_0 = 100$ μM, $[DCF]_0 = 5$ μM, pH = 6, T = 25 ℃

Results and discussion

Degradation of DCF by various oxidants

As shown in Fig. 2, the degradation of DCF was investigated under various oxidation processes, including the PS, PMS, Fe(VI), Fe(VI)/PS, and Fe(VI)/PMS processes. Due to the low reactivity, single PS and PMS systems were almost ineffective for DCF degradation, which was consistent with the researches of Monteagudo et al. (Monteagudo et al. 2018) and Rao et al. (Rao et al. 2018). The removal efficiency of DCF by Fe(VI) alone was 42.2% after 15-min reaction, demonstrating that Fe(VI) alone could partly degrade DCF via 1-e$^-$, 2-e$^-$ or oxygen atom transfer (Lee et al. 2014; Sharma et al. 2015c; Zhao et al. 2018a). In the Fe(VI)/PS process, 10.1% higher removal of DCF was obtained than single Fe(VI), which was mainly caused by the catalysis of Fe^{2+} ions (generated through the decomposition of Fe(VI) (Zhao et al. 2018a; Sheikhi et al. 2022)) for PS to produce more ROSs (sulfate radicals, $SO_4^{\bullet-}$), as indicated by Eq. (3) (Zhen et al. 2012). Actually, the oxidation process of Fe^{2+}-activated PS ($Fe^{2+}/S_2O_8^{2-}$) has gained widespread attention recently and been extensively investigated in water and wastewater remediation due to the superior features and good performances (Zhang et al. 2015; Waclawek et al. 2017; Liu et al. 2018; Nie et al. 2018; Zhen et al. 2018; Gao et al. 2022). Obviously, the DCF degradation was significantly enhanced by the combination of Fe(VI) and PMS with the removal efficiency of 93.5% after 15-min reaction, which was much higher than the sum of Fe(VI) and PMS alone, suggesting a synergistic effect between Fe(VI) and PMS. Owing to the use of phosphate buffer, the solution pH was stable before and after reactions, revealing that the superiority of Fe(VI)/PMS was not attributed to the acidity effect of PMS. Therefore, the synergistic effect between Fe(VI) and PMS, such as the involvement of ROSs, need to be investigated urgently.

$$S_2O_8^{2-} + Fe^{2+} \rightarrow SO_4^{\bullet-} + Fe^{3+} + SO_4^{2-} \quad (3)$$

Effect of initial pH

Indicated by previous studies, the solution pH can greatly affect the stability, oxidation capacity, and existing form of Fe(VI). In the pH range of 4.0–8.0, the self-decomposition of Fe(VI) was accelerated with the decreasing solution pH (Graham et al. 2004; Chen et al. 2018; Liu et al. 2019). The decomposition products and oxidation–reduction potential (E^0) of Fe(VI) are shown as Eqs. (4) and (5) (Sharma 2010). In addition, the pK_a values of Fe(VI) were 1.6, 3.5 and 7.3, respectively, and the four different protonated forms of Fe(VI) were $H_3FeO_4^+$, H_2FeO_4, $HFeO_4^-$, and FeO_4^{2-}, respectively, as shown in Eqs. (6)–(8) (Sharma 2002). The four protonated species of Fe(VI) showed quite different properties.

The effect of solution pH on DCF removal in Fe(VI)/PMS process was investigated, and the results are shown in Fig. 3. After 15-min reaction, 74.7%, 81.9%, 68.1%, 53.2%, and 44.8% DCF degradation efficiencies were obtained at pH 4.0, 5.0, 6.0, 7.0, and 8.0, respectively. The major species of Fe(VI) at pH 4.0–7.0 is $HFeO_4^-$, which self-decomposes rapidly and possesses high reactivity. With the increasing pH (> 7.3), FeO_4^{2-} becomes the major species of Fe(VI), which is more stable but less active than $HFeO_4^-$ (Xu et al.

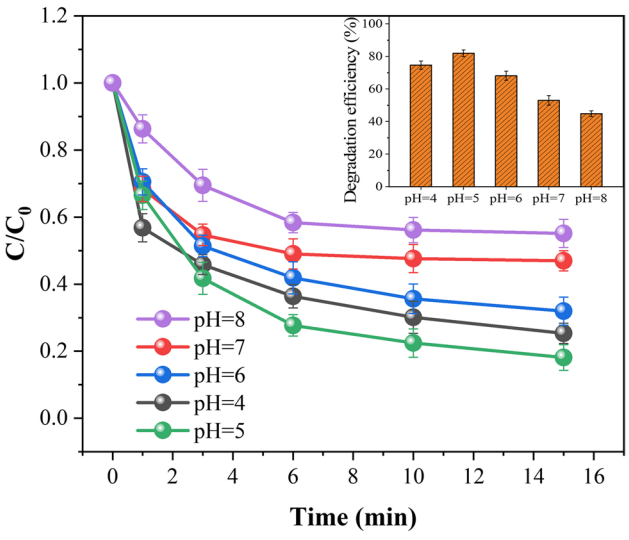

Fig. 3 Effect of initial pH on DCF degradation by Fe(VI)/PMS process. Experimental conditions: $[PMS]_0 = 500$ μM, $[Fe(VI)]_0 = 25$ μM, $[DCF]_0 = 5$ μM, T = 25 ℃

2009; Fei et al. 2022), weakening the activation for PMS and reducing DCF degradation. In addition, it cannot be ignored that the removal efficiency of DCF at pH 4.0 (74.7%) was slightly lower than that at pH 5.0 (81.9%). This result might be owing to that the excess H^+ in strong acidic condition would react with HSO_5^- (the dominant species of PMS) in the pH range of 4.0–8.0 (Mahdi-Ahmed and Chiron 2014) to form hydrogen bonds, which restrained the synergistic effect between Fe(VI) and PMS.

Noticeably, it was recently reported that phosphate buffer inhibits the ferrate oxidation of organic pollutants and disinfection of pathogen due to a complexation between phosphate ions and Fe(V) (formed in the reduction of Fe(VI)) resulting in the reduction of its redox potential (Huang et al. 2018; Manoli et al. 2020). The DCF degradation by Fe(VI)/PMS herein was carried out in phosphate buffer, and thus, the inhibition effect of phosphate ions was not to be ignored. In addition, Huang et al. found that the inhibition effect of phosphate ions strengthened as the concentration increased (Huang et al. 2018). The concentrations of phosphate ions during the DCF degradation by Fe(VI)/PMS process herein are shown in SI Table S2. As can be seen, the concentrations of phosphate ions were 66.67 mM (for solution pH 4.0 and 5.0) and 50 mM (for solution pH 6.0, 7.0 and 8.0), respectively. With the close concentration, phosphate ions showed similar inhibition effects. Regrettably, the actual oxidation capacity of Fe(VI)/PMS was underestimated herein due to the phosphate buffer, and the underlying mechanism warrants further investigation.

Overall, the Fe(VI)/PMS process is efficient for DCF removal in phosphate buffer at pH 4.0–8.0.

$$\text{Acidic media}: FeO_4^{2-} + 8H^+ + 3e- \rightarrow Fe^{3+} + 4H_2O\ E^O = 2.20V \quad (4)$$

$$\text{Basic media}: FeO_4^{2-} + 4H_2O + 3e- \rightarrow Fe(OH)_3 + 5OH^-\ E^O = 0.72V \quad (5)$$

$$H_3FeO_{4^+} \leftrightarrow H^+ + H_2FeO_4, pK_a = 1.6 \pm 0.2 \quad (6)$$

$$H_2FeO_4 \leftrightarrow H^+ + HFeO_4^-, pK_a = 3.5 \quad (7)$$

$$HFeO_4^- \leftrightarrow H^+ + FeO_4^{2-}, pK_a = 7.3 \pm 0.1 \quad (8)$$

Effect of reaction temperature

The effect of reaction temperature on DCF degradation in Fe(VI)/PMS process was investigated in the range of 10–30 ℃. As can be seen in Fig. 4, the removal efficiency of DCF increased with the increasing reaction temperature. Obviously, after 15-min reaction, 70.9% of DCF was degraded at 10 °C, and 80.3% degradation was achieved with the raising temperature to 30 °C. This result might be owing to the following three reasons: (i) the self-decay of Fe(VI) was significantly enhanced by the increase of solution temperature, which generated more active intermediates (Fe(V) and Fe(IV)) and thus promoted the DCF removal (Jiang et al. 2015; Zhao et al. 2018b); (ii) the PMS decomposition was accelerated and more reactive species (such as $SO_4^{\bullet-}$) were generated (Eq. (9)) (Wei et al. 2017; Xiao et al. 2018); (iii) the collision frequencies between DCF and the oxidation species was stepped-up with the increasing temperature.

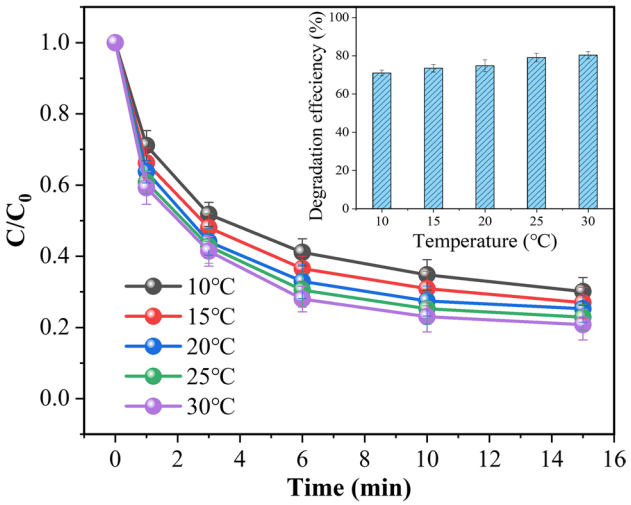

Fig. 4 Effect of reaction temperature on DCF degradation in Fe(VI)/PMS system. Experimental conditions: $[PMS]_0 = 500$ μM, $[Fe(VI)]_0 = 50$ μM, $[DCF]_0 = 5$ μM, pH = 6

$$HSO_5^- \xrightarrow{\Delta} SO_4^{\bullet-} \quad (9)$$

To further explore the impact of solution temperature, the self-decomposition of Fe(VI) with the solution temperature range from 10 to 30 ℃ was investigated, and the results are shown in Fig. 5. The pseudo-first-order rate constant (k_{obs}) of Fe(VI) decomposition increased from 0.0029 (10℃) to 0.0081 min^{-1} (30 ℃), and the activation energy (E_a) for the reaction was calculated to be 34.9695 $kJ{\cdot}mol^{-1}$, which revealed the great dependence for the property of Fe(VI) on reaction temperature.

Effect of Fe(VI) and PMS doses

The effects of Fe(VI) and PMS doses on DCF degradation are shown in Fig. 6. As the dosage of Fe(VI) increased from 6.25 to 100 μM, the removal efficiency of DCF was significantly enhanced from 17.8 to 93.2% within 15-min reaction (Fig. 6a). There might be two reasons for it: (i) Fe(VI) itself could effectively oxidize and degrade DCF due to its high

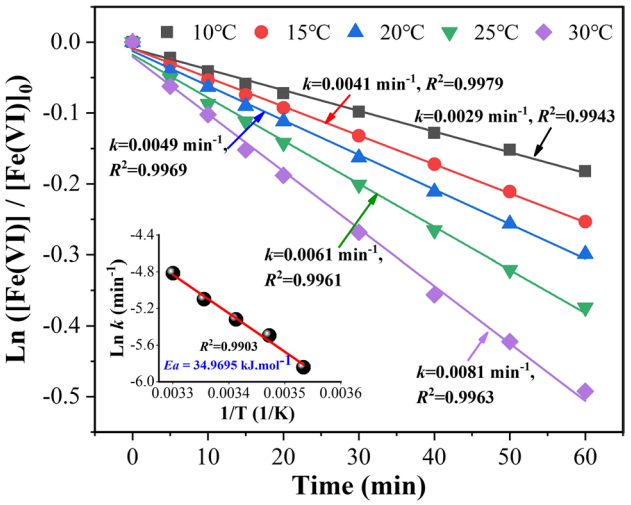

Fig. 5 Effect of temperature on the self-decomposition of Fe(VI). Experimental conditions: $[Fe(VI)]_0 = 50$ μM, pH = 6

oxidizability and self-catalysis by the reactive byproducts (i.e., Fe(III) and Fe(II) ions), as demonstrated in our previous research (Zhao et al. 2018a) and (ii) more Fe(III) and Fe(II) ions were generated from the larger amount of Fe(VI), which could active PMS to produce more reactive species (such as $SO_4^{\bullet-}$) and thus accelerated the degradation of DCF.

Figure 6b shows the effects of PMS dosages on DCF degradation. When the dosages of PMS were 50, 250, 500, and 1000 μM, the removal rates of DCF were 51.09%, 65.09%, 77.15% and 91.21%, respectively. The increase was mostly caused by the abundant reactive species generated from the activation of sufficient PMS (Ding et al. 2020). The phenomenon was reported in previous researches (Ghanbari and Moradi 2017; Chen et al. 2022b). However, the degradation efficiency of DCF was slightly reduced with the excessive addition of PMS (2000 μM), which was resulted by the quenching reaction between PMS and reactive species (i.e., $^{\bullet}OH$ and $SO_4^{\bullet-}$), as shown in Eqs. (10) and (11) (Wang et al. 2020).

$$HSO_5^- + {}^{\cdot}OH \rightarrow SO_5^{\cdot-} + H_2O \quad k = 1.7 \times 10^7 M^{-1}s^{-1} \quad (10)$$

$$HSO_5^- + SO_4^{\cdot-} \rightarrow SO_5^{\cdot-} + SO_4^{2-} + H^+ \quad k < 10^5 M^{-1}s^{-1} \quad (11)$$

Effect of inorganic anions and humic acid

As shown in Fig. 7a–c, the effects of inorganic anions (HCO_3^-, Cl^-, NO_3^- and SO_4^{2-}) on DCF degradation in Fe(VI)/PMS system were investigated. As seen in Fig. 7a, the existence of 4 mM NO_3^- and SO_4^{2-} showed almost no effect on DCF removal, which is in accordance with bisphenol A removal by CuO/Fe_3O_4-PMS (Ding et al. 2020). However, Hu and Luo (Luo et al. 2017; Hu et al. 2018) reported that excess NO_3^- and SO_4^{2-} would quench active radicals, such as $SO_4^{\bullet-}$ and $^{\bullet}OH$, and then showed inhibitory effects.

In addition, the same dosage of Cl^- and HCO_3^- (4 mM) showed noticeable inhibition effects on DCF removal by Fe(VI)/PMS process. As presented in Fig. 7b, the degradation efficiency of DCF after 15-min reaction was decreased from 77.15 to 47.88% with the absence of 8 mM Cl^-. It was previously inferred that Cl^- as a vital scavenger for $SO_4^{\bullet-}$ and $^{\bullet}OH$ to generate $Cl^{\bullet}$ and $Cl_2^{\bullet-}$ (Eqs. (12)-(17)),

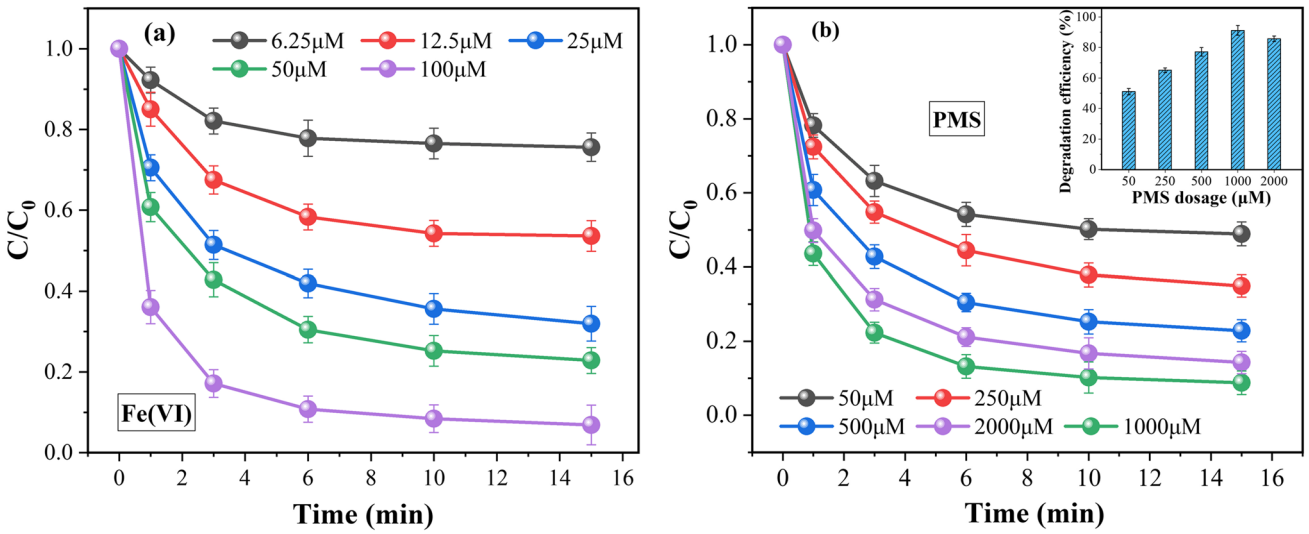

Fig. 6 Effect of oxidants dosage on the degradation of DCF in Fe(VI)/PMS system. Experimental conditions: $[DCF]_0 = 5$ μM, pH = 6, T = 25℃; for (**a**) $[PMS]_0 = 500$ μM; for (**b**) $[Fe(VI)]_0 = 50$ μM

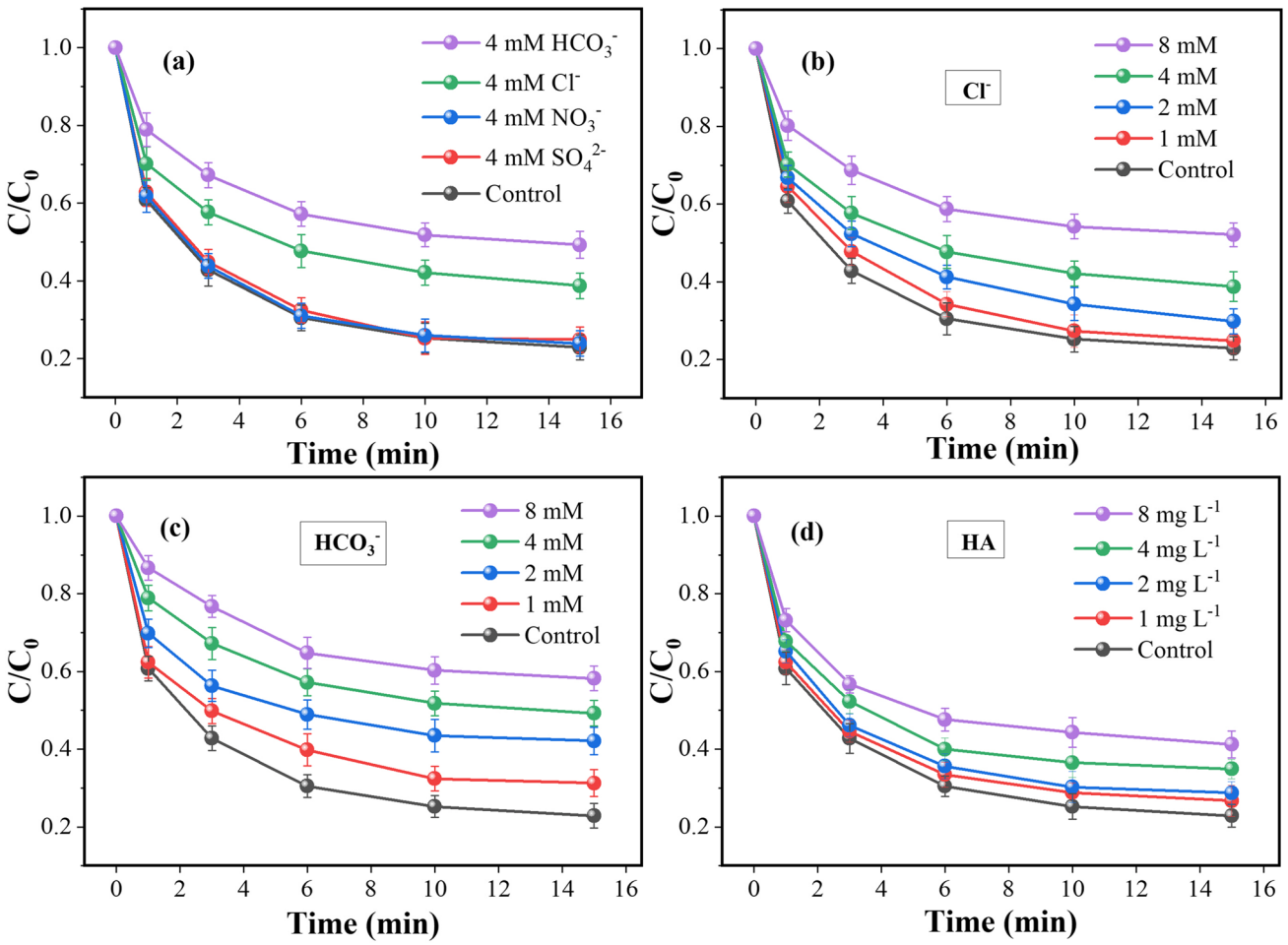

Fig. 7 Effect of inorganic anions (HCO_3^-, Cl^-, NO_3^-, SO_4^{2-}) and humic acid on DCF degradation in Fe(VI)/PMS system. Experimental conditions: $[DCF]_0 = 5$ μM, $[Fe(VI)]_0 = 50$ μM, $[PMS]_0 = 500$ μM, pH = 6, T = 25 ℃

which possess lower reactivity (Chan and Chu 2009; Wang et al. 2011; Ding et al. 2020; Yang et al. 2022). Hence, the consumption of $SO_4^{\bullet-}$ and $^{\bullet}OH$ by Cl^- restrained the DCF degradation, which corresponding well to the decay of iopamidol and X-ray contrast medium by UV/sulfite, UV/chlorine, and UV/H_2O_2, respectively (Kong et al. 2018; Cao et al. 2021). Interestingly, previous studies showed that acid conditions were conductive to the formation of $Cl_2^{\bullet-}$ (Wu et al. 2019), whereas the consumption of $^{\bullet}OH$ by Cl^- under alkaline conditions can be ignored due to the reversible reaction between Cl^- and $^{\bullet}OH$ (Yang et al. 2014). To sum up, the existence of Cl^- was adverse for DCF degradation in Fe(VI)/PMS process under this experimental condition.

As shown in Fig. 7c, the addition of 8 mM HCO_3^- reduced DCF removal efficiency from 77.15 to 41.79%. The inhibition effect of HCO_3^- mainly attributed to the quenching of $SO_4^{\bullet-}$ and $^{\bullet}OH$ (Eqs. (18) and (19)), which generated carbonate radicals ($CO_3^{\bullet-}$ and $HCO_3^{\bullet}$) with weaker oxidization ability (Zuo et al. 1999; Sharma et al. 2015b; Chen et al. 2022b, a; Yang et al. 2022). Impressively, Luo et al. found the obviously enhanced effect of HCO_3^- on pharmaceutical degradation by Fe(VI), which is a significant contrast to the strong scavenging effect of HCO_3^- (Luo et al. 2019). It was very likely that HCO_3^- can stabilize the intermediate Fe(V) species produced from Fe(VI) via complexation, reducing redox potential and prolonging Fe(V)'s lifetime, thereby preventing rapid spontaneous self-decomposition of Fe(V) and facilitating oxidation rate of pharmaceuticals. In addition, previous studies have shown higher stability of Fe(V)-carbonate complex than that of Fe(V)-pyrophosphate complex (Bielski 1990; Melton and Bielski 1990). And regrettably, phosphate was used as buffer in this study, and the enhanced effect of HCO_3^- was significantly concealed by the complexation of Fe(V) with phosphate. The inhibitive effect of phosphate ions on Fe(V) oxidation led to the outcompeting of Fe(V) autodecomposition pathway and finally debilitating the overall oxidation capacity of Fe(VI) (Huang et al. 2018).

$$Cl^- + SO_4^{\bullet-} \rightarrow Cl^{\bullet} + SO_4^{2-} \quad k = (2.7-6.6)\times 10^8 M^{-1}s^{-1} \quad (12)$$

$$Cl^- + Cl^{\bullet} \rightarrow Cl_2^{\bullet-} \quad k = 8.5\times 10^9 M^{-1}s^{-1} \quad (13)$$

$$Cl_2^{\bullet-} + Cl_2^{\bullet-} \rightarrow 2Cl^- + Cl_2 \quad k = 9\times 10^6 M^{-1}s^{-1} \quad (14)$$

$$Cl_2^{\bullet-} + Cl^{\bullet} \rightarrow Cl_2 + Cl^- \quad k = 4.3\times 10^9 M^{-1}s^{-1} \quad (15)$$

$$Cl^- + {}^{\bullet}OH \rightarrow OHCl^{\bullet-} \quad k = 4.3\times 10^9 M^{-1}s^{-1} \quad (16)$$

$$OHCl^{\bullet-} + H^+ \rightarrow Cl^{\bullet} + H_2O \quad k = 2.1\times 10^{10} M^{-1}s^{-1} \quad (17)$$

$$HCO_3^- + {}^{\bullet}OH \rightarrow CO_3^{\bullet-} + H_2O \quad k = 8.5\times 10^6 M^{-1}s^{-1} \quad (18)$$

$$HCO_3^- + SO_4^{\bullet-} \rightarrow HCO_3^{\bullet} + SO_4^{2-} \quad k = 9.1\times 10^6 M^{-1}s^{-1} \quad (19)$$

Natural organic matter (NOM) is one of the major constituents in water resource. Thereby, its necessary to explore the influence of NOM on organic pollutant degradation in Fe(VI)/PMS system. In this study, humic acid (HA) was used as a probe to evaluate the effect of NOM on DCF degradation, and the results are shown in Fig. 7d. The DCF removal decreased with the increasing addition of HA. When the addition of HA increased from 0 to 8 mg L^{-1}, the DCF degradation efficiency reduced obviously from 77.15 to 58.78% after 15-min reaction, respectively. The inhibiting effect of HA was ascribed to the competitive reaction with the major free radicals (i.e., $SO_4^{\bullet-}$ and $^{\bullet}OH$), which mainly occurred in the electron-rich sites of HA (Gara et al. 2009). The similar results were detected during atrazine degradation by Fe(VI)/PMS process (Wu et al. 2018b) and bisphenol A removal by CuO/Fe_3O_4-PMS process (Ding et al. 2020).

Reactive species and possible degradation mechanisms

To investigate the reaction mechanism and reactive species in Fe(VI)/PMS system, the classical radical quenching experiments using methanol (MeOH) and *tert*-butanol (TBA) as scavengers were conducted (Fig. 8a). It is well accepted that MeOH can effectively scavenge both $SO_4^{\bullet-}$ and $^{\bullet}OH$ with the reaction rate constants of $0.9–1.3\times 10^7$ M^{-1} s^{-1} and $8–10\times 10^8$ M^{-1} s^{-1}, respectively (Eibenberger et al. 1978). And TBA possess similar excellent reactivity with $SO_4^{\bullet-}$ and $^{\bullet}OH$ ($k_{SO4^{\bullet-}/TBA} = 4–9.1\times 10^5$ M^{-1} s^{-1}, $k_{^{\bullet}OH/TBA} = 3.8–7.6\times 10^8$ M^{-1} s^{-1}) (Anipsitakis and Dionysiou 2004). As can be seen in Fig. 8a, both MeOH and TBA can obviously inhibit the DCF degradation in Fe(VI)/PMS process. With the addition of 10 mM MeOH and TBA, DCF removal efficiency decreased to 35.12% and 45.22% within 6-min reaction, respectively, and then remain almost stable. As the dosages of MeOH and TBA increased to 50 mM, the degradation efficiency of DCF reduced to 26.33% and 32.18% after 6-min reaction, respectively. The above results indicated that $SO_4^{\bullet-}$ and $^{\bullet}OH$ might be the main reactive species responsible for DCF removal in Fe(VI)/PMS system. Of note is that, however, MeOH could scavenge high-valent iron intermediates ($k = 5.72\times 10^2$ $M^{-1}\cdot s^{-1}$), whereas the quenching effect of TBA on high-valent iron intermediates ($k = 6\times 10^1$ $M^{-1}\cdot s^{-1}$) is much lower than that of MeOH (Oleg and Andreja 2004), which also suggested the role of Fe(IV)/Fe(V) in the DCF degradation and explained why the inhibition of MeOH was little stronger than that of TBA.

To further verify the reactive species, EPR experiments were introduced using DMPO as a spin-trapping agent. As shown in Fig. 8b, no obvious signals of $SO_4^{\bullet-}$ and $^{\bullet}OH$ radicals were captured in the pure Fe(VI) or PMS process. In Fe(VI)/PMS system, obvious signals of $SO_4^{\bullet-}$ and $^{\bullet}OH$ radicals were observed, indicating that Fe(VI) and the intermediate products (such as Fe(II) or Fe(III)) could activate PMS to produce a certain amount of $SO_4^{\bullet-}$ and $^{\bullet}OH$ radicals. It was consistent with the quenching experiment results. The above results showed that $SO_4^{\bullet-}$ and $^{\bullet}OH$ radicals were involved in DCF removal by Fe(VI)/PMS process, which was consistent with the research results of Wu et al. (Wu et al. 2018b).

It has been well demonstrated that methyl phenyl sulfoxide (PMSO) is a good probe for identifying Fe(IV)/Fe(V), because it can be oxidized by Fe(IV)/Fe(V) to produce methyl phenyl sulfone ($PMSO_2$) through an oxygen-atom transfer step, which is markedly different from the radicals-based oxidation pathway (Jin et al. 2022; Zhu et al. 2020). To further confirm the involvement of Fe(V)/Fe(IV) species in DCF degradation by Fe(VI)/PMS process, PMSO was applied as the probing agent in this study, and the PMSO consumption and $PMSO_2$ generation were observed. As shown in Fig. 8c and d, PMS can promote Fe(VI) to oxidize PMSO. Specifically, the removal efficiency of PMSO in Fe(VI) alone and Fe(VI)/PMS systems are 29.11% and 48.05% after 15-min reaction, respectively, meaning that with the existence of PMS more high-valent Fe intermediates were generated. In addition, the molar ratios of generated $PMSO_2$ to oxidized PMSO (i.e., $\Delta[PMSO_2]/\Delta[PMSO]$) were 65.17% and 64.79% in Fe(VI) alone and Fe(VI)/PMS systems (Fig. 8c and d), respectively, further proving the existence of Fe(IV)/Fe(V). Yang et al. revealed that the main species for PMSO degradation would gradually convert from Fe(IV)/Fe(V) to $SO_4^{\bullet-}$/HO• with the dosage of sulfite increasing from 50 μM to 600 μM, and thus reduced the molar ratio of $\Delta[PMSO_2]/\Delta[PMSO]$ (Yang et al. 2022). It could be inferred that the PMSO consumption and $PMSO_2$ generation in this study were disturbed by the abundant active species ($SO_4^{\bullet-}$/HO•) formed by the PMS

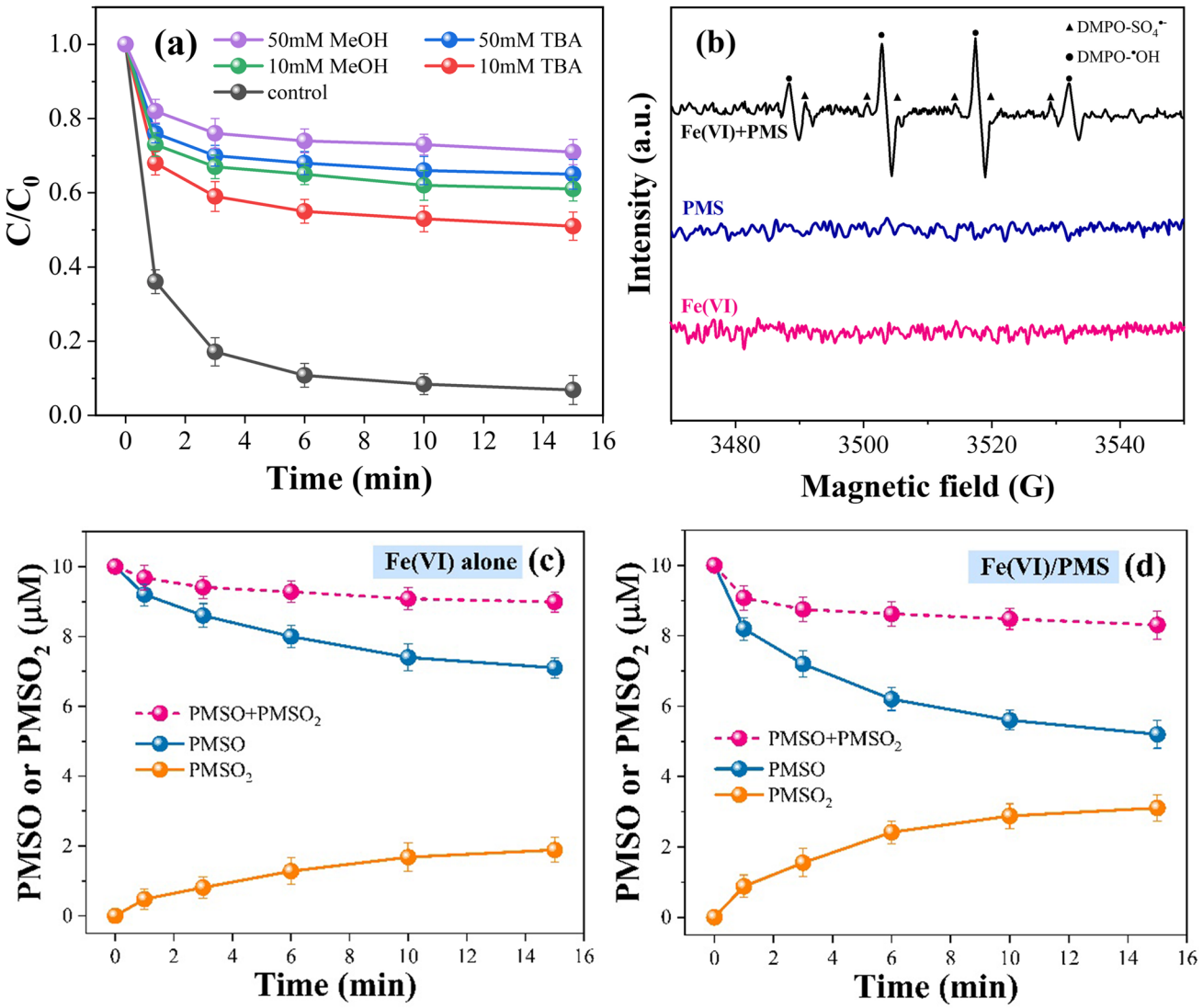

Fig. 8 **a** Effect of radical scavengers on DCF degradation in Fe(VI)/PMS system. **b** EPR spectra of different systems obtained in DMPO-H_2O solution. PMSO removal and $PMSO_2$ production in **c** the Fe(VI) system and **d** the Fe(VI)/PMS system. Experimental conditions: $[DCF]_0 = 5$ μM, $[Fe(VI)]_0 = 100$ μM, $[PMS]_0 = 500$ μM, $[DMPO]_0 = 10$ mM, $[PMSO]_0 = 10$ μM, pH = 6, T = 25 ℃

activation. Beyond that, previous studies revealed that the phosphate buffer used in this study would decrease the reactivity of Fe(V) species and thus debilitate the overall oxidation capacity of ferrate (Shao et al. 2019; Huang et al. 2021). Huang et al. investigated the impact of phosphate on ferrate oxidation of organic compounds and found that phosphate anions (50 mM, pH = 6, herein) may complex with Fe(V) species and decrease its reactivity due to redox potential reduction or steric effect (Huang et al. 2018). Therefore, the actual oxidation ability of ferrate for PMSO might be underestimated herein. To sum up, $SO_4^{\bullet-}$, HO•, and Fe(IV)/Fe(V) were involved in DCF removal by Fe(VI)/PMS process.

Previous studies explored the generation of Fe(V), Fe(IV), Fe(III), and Fe(II) during the reaction of Fe(VI) with organic pollutants through 1-e^- and 2-e^- transfer processes (Sharma 2011, 2013; Lee et al. 2014; Chen et al. 2022a). Meanwhile, the dissolved iron ions (in situ Fe(III) and Fe(II)) could efficiency active Fe(VI) and PMS to produce more actives species (such as Fe(V)/Fe(IV), $SO_4^{\bullet-}$/HO•) (Eqs. (20)–(22)) (Feng et al. 2017; Cheng et al. 2017; Wu et al. 2018b; Shao et al. 2019; Zhu et al. 2020; Sharma et al. 2022). To further confirm the reaction mechanisms of Fe(VI)/PMS system, the concentration variations of PMS and iron ions in solution were monitored (Fig. 9). As shown in Fig. 9, the concentration of PMS decreased rapidly to 377 μM within the first 3 min, and remained stable thereafter, which corresponded well to the degradation of DCF in Fe(VI)/PMS system. The concentrations of Fe(III) and Fe(II) increased to 14 μM and 9 μM within 3 min, respectively, and then rapidly decreased, which was well consistent with the decomposition of PMS

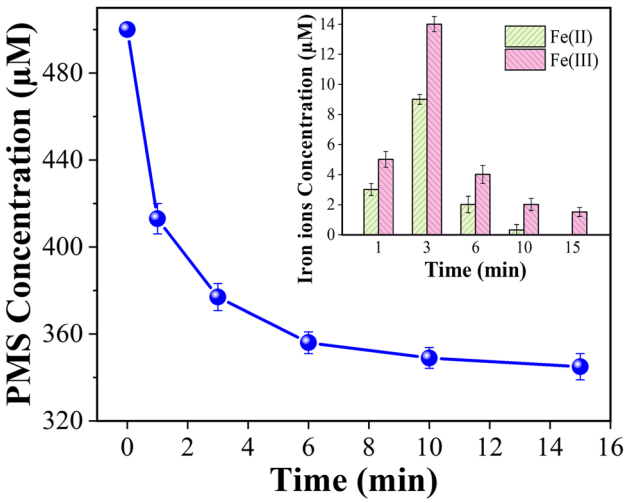

Fig. 9 Concentration of PMS and iron ions as a function of time. Experimental conditions: $[DCF]_0 = 5$ μM, $[Fe(VI)]_0 = 100$ μM, $[PMS]_0 = 500$ μM, pH = 6, T = 25 ℃

and DCF. The above results indicated the involvement of dissolved iron ions (Fe(III) and Fe(II)) for the DCF removal in Fe(VI)/PMS system.

$$Fe^{3+} + HSO_5^- \rightarrow Fe^{2+} + SO_5^{\bullet-} + H^+ \quad (20)$$

$$Fe^{2+} + HSO_5^- \rightarrow Fe^{3+} + SO_4^{\bullet-} + OH^- \quad (21)$$

$$SO_4^{\bullet-} + H_2O \rightarrow SO_4^{2-} + {}^{\bullet}OH + H^+ \quad (22)$$

On the basis of the above discussion and results, the reaction mechanism of Fe(VI)/PMS system is proposed and illustrated in Scheme 1. On one hand, Fe(VI) would decompose rapidly to Fe(V) and Fe(IV) in acidic solution through 1-e^- and 2-e^- transfer processes. Thus, DCF could be directly degraded by Fe(VI), Fe(V), and Fe(IV) with strong oxidation property. On the other hand, Fe(III), the by-products from the self-decomposition of Fe(VI) could active PMS to produce $SO_5^{\bullet-}$ and Fe(II) (Eq. (20)). Then Fe(II) could react with PMS to generate $SO_4^{\bullet-}$ and Fe(III) (Eq. (21)), thus forming the iron cycle between Fe(III) and Fe(II). Subsequently, $SO_4^{\bullet-}$ reacted with H_2O to produce ${}^{\bullet}OH$ (Eq. (22)). In addition, Fe(III) and Fe(II) could catalyze Fe(VI) to generate more Fe(V) and Fe(IV) and thus resulted in highly effective DCF degradation. In summary, the above results showed that free radicals ($SO_4^{\bullet-}$ and ${}^{\bullet}OH$) and non-radicals (Fe(VI), Fe(V) and Fe(IV)) coexist in the Fe(VI)/PMS system.

Removal of TOC

The removal efficiency of TOC is a critical indicator for evaluating the quality of treated water and effectiveness of water treatment process. As can be seen in Fig. 10, compared with Fe(VI) oxidation, Fe(VI)/PMS process is more effective for the DCF degradation and TOC removal in the system. As shown in Fig. 10a, 42.13% DCF and 34.79% TOC were removed within 15-min reaction by Fe(VI) in the filtered samples. Under the same condition, 93.15% DCF and 63.79% TOC were removed in Fe(VI)/PMS system. This indicates that the coupling effects of Fe(VI)/PMS process, such as accelerating the formation of active species ($SO_4^{\bullet-}$ and ${}^{\bullet}OH$) (Eqs. (20)–(22)), played an important role for the DCF degradation and TOC removal.

Previous studies reported that the ferric particles (composing by Fe2O3, FeOOH, and amorphous ferric), which were formed in the reduction of Fe(VI), possessed great adsorption potential for the removal of organics (Liu et al. 2017b; Yang et al. 2018a, 2018b; Tian et al. 2020). To further explore the TOC removal mechanism, the variations of TOC removal ratio in filtered and acidified samples by Fe(VI) and Fe(VI)/PMS processes were investigated (Fig. 10b). The filtered

Scheme 1 Reaction mechanism of DCF degradation in Fe(VI)/PMS system

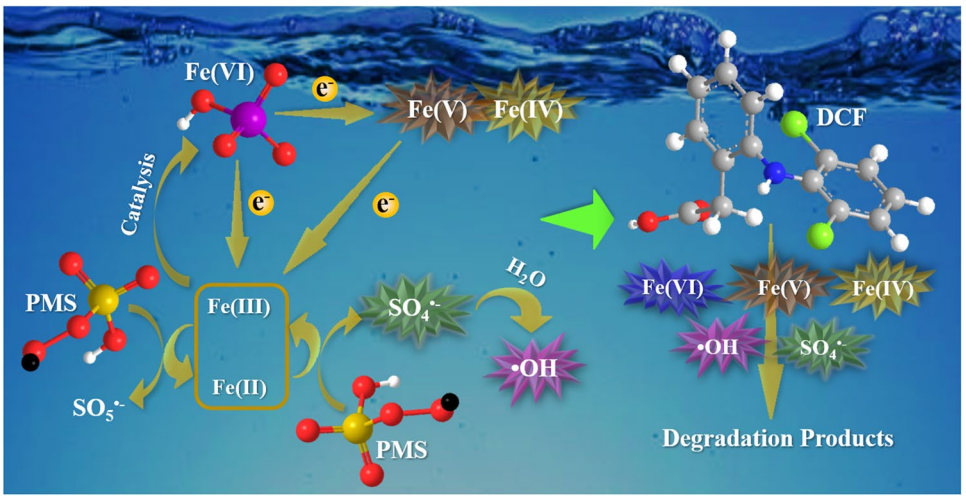

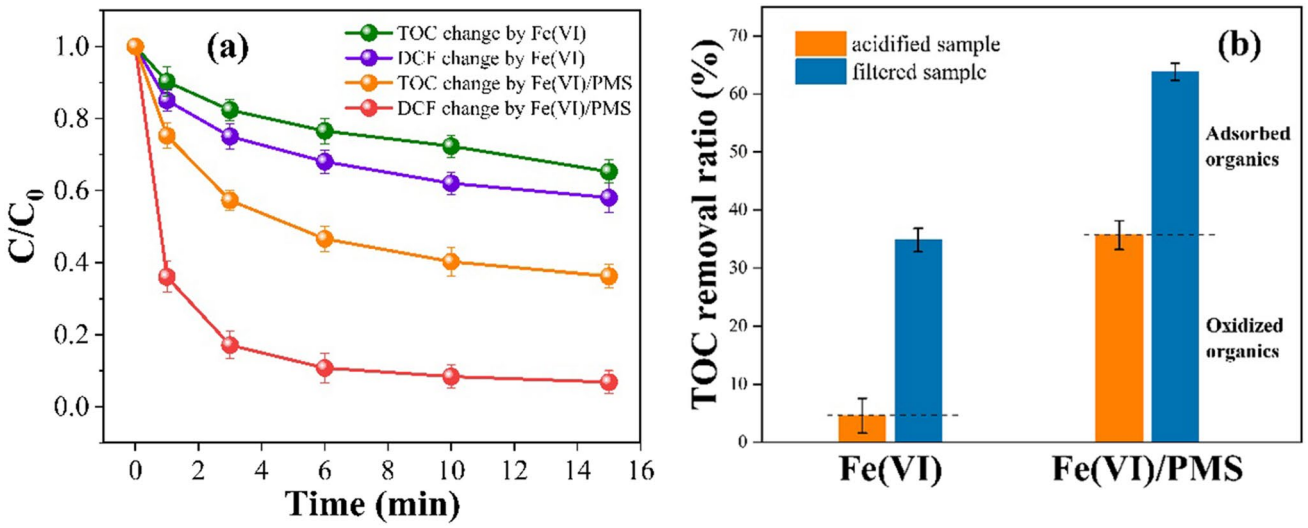

Fig. 10 **a** DCF degradation and TOC variations in filtered samples by Fe(VI) and Fe(VI)/PMS processes. **b** The variations of TOC removal ratio in filtered and acidified samples. Experimental conditions: $[DCF]_0 = 5$ μM, $[Fe(VI)]_0 = 100$ μM, $[PMS]_0 = 500$ μM, pH = 6, T = 25 ℃

samples indicates that the solution samples were filtered through 0.22-μm glass fiber filter to remove ferric particles, and the acidified samples indicates that the solution samples (ferric solids) were dissolved with 0.5% of HCl, which represents the actually eliminated TOC in Fe(VI) oxidation process. Obviously, the TOC removal ratio was largely reduced in acidified samples than those in filtered samples (Fig. 10b). In the acidified samples, 4.56% and 35.65% TOC were eliminated by Fe(VI) and Fe(VI)/PMS processes, respectively. Compared with the oxidized organics, ferric particles acted as adsorbent and removed around 30% of TOC in the processes. Hence, the removal of DCF and TOC in Fe(VI) and Fe(VI)/PMS systems was a complex process, and both oxidation and adsorption were functioned in the removal process.

Degradation intermediates and possible decay pathways of DCF

The reaction intermediates of DCF in Fe(VI)/PMS process were identified by UPLC-QTOF/MS. As shown in Scheme 2, sixteen oxidation products (OPs) were detected and their chemical structure were deduced. The mass to charge ratio (*m/z*), retention time (RT), and formula of the OPs are exhibited in Table S3 in SI, and their relative formation and evolution with the reaction time are exhibited in Fig. S1(a) and (b). Based on previous studies about DCF oxidation (Zhang et al. 2022; Zhao et al. 2022a, b), and the chemical structure of OPs in this study, eight possible degradation pathways of DCF in Fe(VI)/PMS process were proposed, including hydroxylation, decarboxylation, ring closure, dehydrogenation, C-N bond cleavage, formylation, dichlorination-hydroxylation, and sulfonation.

(1) Hydroxylation (pathway (1) in Scheme 2) is a common reaction pathway in Fe(VI)/PMS process. The by-products *m/z* 311and *m/z* 327 were generated by the addition of •OH at the unsaturated C5 = C6 and C3' = C4' successively. And these two products were frequently detected in DCF oxidation (Chi et al. 2022). Another hydroxylated product *m/z* 282 was formed by the •OH addition at the C5 = C6 of *m/z* 266 (isomer-1), which was produced by formylation.

(2) Decarboxylation (pathway (2) in Scheme 2) meant the loss of carboxyl group ($-CO_2$) from acetoxy group ($-CH_2COOH$), and then formed methyl at C1. The OPs *m/z* 252, *m/z* 266 (isomer-2) and *m/z* 122 were all produced by decarboxylation, which was mainly caused by the attack of $SO_4^{\bullet-}$ and •OH on the lateral chain of DCF. Other decarboxylation OPs, such as 2-((2′,6′-dichlorophenyl) amino) methylbenzene ($C_{13}Cl_2NH_{11}$, *m/z* 252), 2-((2′,6′-dichlorophenyl) amino) m-methylphenol ($C_{13}Cl_2NOH_{11}$, *m/z* 268), and 2-((2′,6′-dichlorophenyl) amino)-4′,5-dihydroxy-benzyl alcohol ($C_{13}Cl_2NO_3H_{11}$, *m/z* 300) were detected during the DCF degradation in heterogeneous activation of PMS by $LaFeO_3$ (Rao et al. 2018), photo-electrocatalysis of Cu/PS (Liu et al. 2017a) and a like Fenton system of $FeCeO_x$-H_2O_2 (Chong et al. 2017), respectively.

(3) Ring closure (pathway (3) in Scheme 2) referred to the loss of HCl (-36D) and further structural rearrangement or intramolecular reaction of DCF. The detected product *m/z* 259 was formed by this path in this study. And it was also observed during the DCF degradation by the combining use of manganese oxide octahedral molecular sieve with PMS (P2) (Wu et al. 2018a),

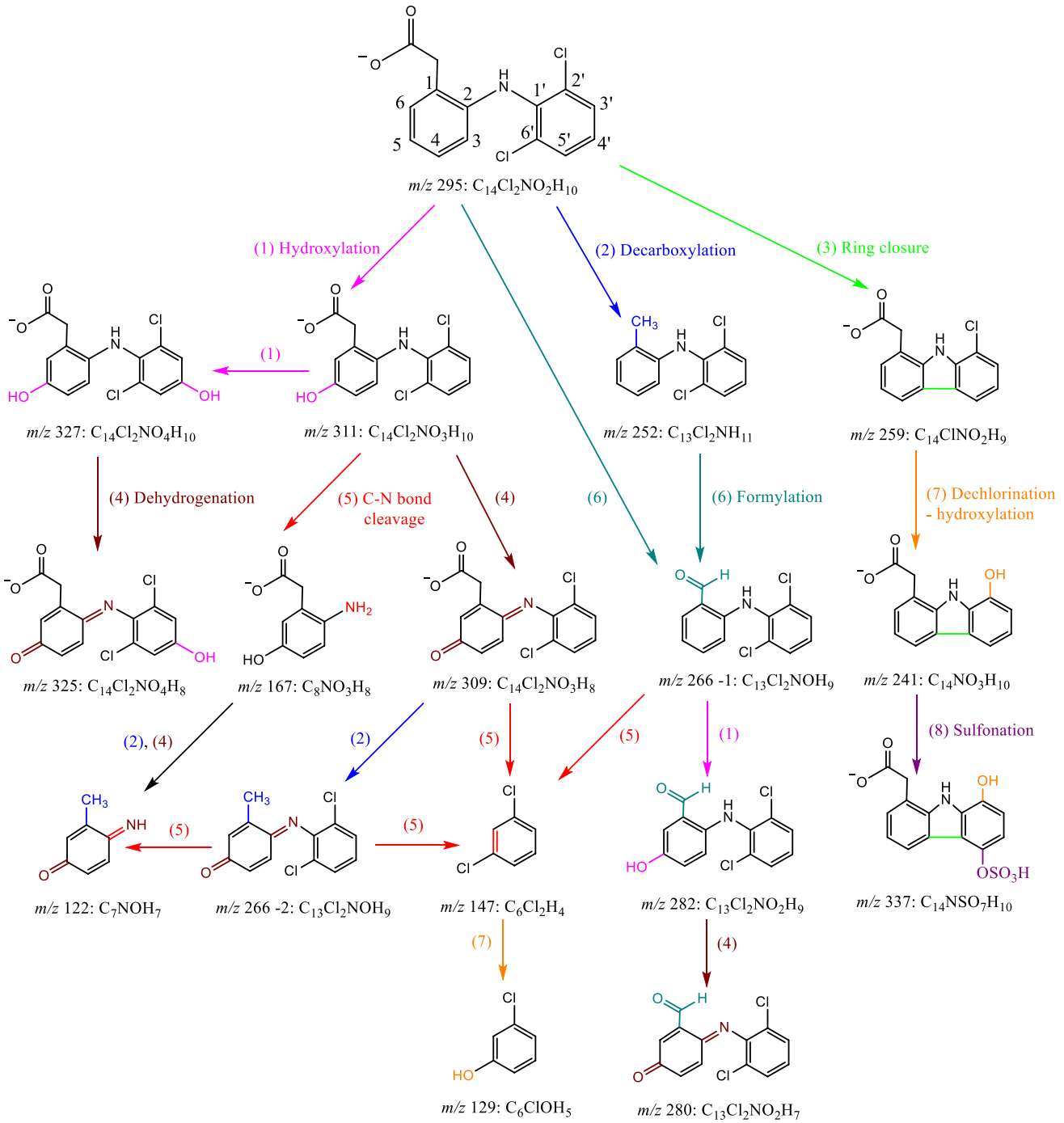

Scheme 2 Proposed degradation intermediates and reaction pathways of DCF in Fe(VI)/PMS process: (1) hydroxylation, (2) decarboxylation, (3) ring closure, (4) dehydrogenation, (5) C-N bond cleavage, (6) formylation, (7) dechlorination-hydroxylation, (8) sulfonation. Experimental conditions: $[DCF]_0 = 5$ μM, $[Fe(VI)]_0 = 100$ μM, $[PMS]_0 = 500$ μM, pH = 6, T = 25 ℃

the hydroxyl radical-mediated oxidation process (P4) (Agopcan Cinar et al. 2017), and the heterogeneous photocatalysis using nanostructured TiO_2 (P1) (Martínez et al. 2011). These findings suggest that the ring closure of DCF was resulted by the attack of •OH.

(4) Dehydrogenation (pathway (4) in Scheme 2) was an important reaction path generally following the hydroxylation of DCF. Since hydroxylation resulted −OH addition at the *para*-position of $-NH_2$, the electronic density of the aromatic ring was changed. In this study,

the all hydroxylation products (*m/z* 311, *m/z* 327, *m/z* 282 and *m/z* 167) possessed high electronic density in the *ortho*- and *para*-positions of the aromatic ring with −OH and $-NH_2$ acting as the electron-donating groups (Zhou and Jiang 2015). Fe(VI) or the intermediates (i.e., Fe(V) and Fe(IV)) could readily attack these sites and then generated *m/z* 309, *m/z* 325, *m/z* 280 and *m/z* 122.

(5) C-N bond cleavage (pathway (5) in Scheme 2) resulted by the attack of Fe(VI), $SO_4^{\bullet-}$ and $^{\bullet}OH$ at the *ipso*-position of $-NH-$ or $=N-$ leading to the cleavage of the C-N bond. Four C-N bond cleavage OPs were detected in this study, including *m/z* 167, *m/z* 122, *m/z* 147 and *m/z* 129. Also, similar C-N bond cleavage OPs were observed in DCF removal by simulated solar assisted photocatalysis (Salaeh et al. 2016), aqueous chlorine dioxide (Wang et al. 2014), and ultrasonic persulfate process (US/PS) (Monteagudo et al. 2018).

(6) Formylation (pathway (6) in Scheme 2) meant the formation of formoxyl at the C1 site of DCF. The detected formylation product *m/z* 266 (isomer-1) might result from two different ways. For one, the acetoxy group ($-CH_2COOH$) at the C1 site of DCF was attacked directly to formoxyl. For another, DCF firstly suffered the decarboxylation oxidizing the acetoxy group to methyl (*m/z* 252, reaction pathway (2)), and subsequently *m/z* 252 was further oxidized converting the methyl to formoxyl. This product was also documented in other advanced oxidation systems, such as the DCF degradation by $LaFeO_3$/PMS (compound 4) (Rao et al. 2018), and the DCF removal by $FeCeO_x$-H_2O_2 (2-(2,6-dichlorophenylamino) benzaldehyde) (Chong et al. 2017).

(7) Dechlorination-hydroxylation (pathway (7) in Scheme 2) referred to the substitution of chlorine in benzene ring by hydroxyl group (-18D). Two OPs *m/z* 241 and *m/z* 129 were resulted by dechlorination-hydroxylation in this study. Coelho et al. (Coelho et al. 2009) and Salaeh et al. (Salaeh et al. 2016) both observed similar product, 2-amino-3-chloro-phenol (C_6ClNOH_6, *m/z* 179), during the DCF oxidation by ozonation and photocatalysis, respectively.

(8) Sulfonation (pathway (8) in Scheme 2) was resulted by the attack of $SO_4^{\bullet-}$ leading to the attachment of $-OSO_3H$ to the C5' site of benzene ring. Same product *m/z* 337 (in this study) was also detected by Rao et al. (Rao et al. 2018).

Toxicity analysis

Several previous studies have pointed out that the toxicity of aqueous solutions may increase due to the generation of some highly toxic aromatic compounds during the degradation of pollutants (Zhang et al. 2022, 2021). Therefore, it is essential to assess the toxicity characteristics of DCF and the degradation intermediates during the Fe(VI)/PMS process. ECOSAR software was utilized to predict the acute toxicity (LC_{50} or EC_{50}) and chronic toxicity (ChV) of DCF and its intermediates (Fig. 11 and Table S4).

According to the system established by the Globally Harmonized System of Classification and Labeling of Chemicals (GHS), the predicted toxicity values of DCF and its intermediates can be divided into four categories: very toxic (LC_{50}/EC_{50}/ ChV < 1 mg/L), toxic (1 mg/L < LC_{50}/EC_{50}/ChV < 10 mg/L), harmful (10 mg/L < LC_{50}/EC_{50}/ChV < 100 mg/L), and not harmful (LC_{50}/EC_{50}/ChV > 100 mg/L). The values of $LC_{50,96\ h}$ (fish), $LC_{50,48\ h}$ (daphnid), and $EC_{50,96\ h}$ (green algae) for DCF were 37.655, 25.754, and 41.414 mg·L^{-1}, respectively. The acute toxicity of DCF was classified as "harmful" to fish, daphnid, and green algae, while the chronic toxicity of DCF was classified as "toxic" to fish and daphnid. The degradation intermediates m/z 266–1, m/z 252, m/z 129, m/z 280, m/z 147, m/z 266–2, m/z 282 present higher acute toxicity and chronic toxicity than DCF. Among them, the intermediates m/z 266–1 and m/z 252 were worthy of more attention because of high predicted acute and chronic toxicity (both classified as "very toxic" to fish and daphnid). However, with the prolongation of degradation time, the conversion products of m/z 266–1 and m/z 252 through different pathways, m/z 282 (pathway (1)) and m/z 147 (pathway (5)), presented lower acute and chronic toxicity. The intermediates m/z 259, m/z 311, m/z 337, m/z 167, m/z 122, m/z 325, m/z 241, and m/z 309 were less toxic than DCF, and some of them became "not harmful," which can result in the reduction in ecotoxicity of the reacted solution. As shown in Fig. S1, the intermediate products were further degraded in the Fe(VI)/PMS process as the reaction progressed, thereby decreasing both acute toxicity and chronic toxicity. The toxicity of the reaction solution depends on not only the characteristics of the intermediate products, but also their concentrations. Due to a lack of standard materials, this issue could not be addressed in this research and will conduct an in-depth study on this issue.

Removal of DCF in real waters

To explore the practical application of the Fe(VI)/PMS process, the ultra-pure water and four different natural water samples were collected and used as water background matrices in this study. The properties of the water samples are exhibited in Table S5. As can be seen in Fig. 12, the DCF degradation in tap water was slightly reduced (90.17%) due to the higher pH and TOC concentration than that in ultra-pure water (95.72%) within 30-min reaction. In the 1#, 2# river water, and lake water, the degradation efficiency of DCF were obviously decreased to 66.81%, 78.14%, and

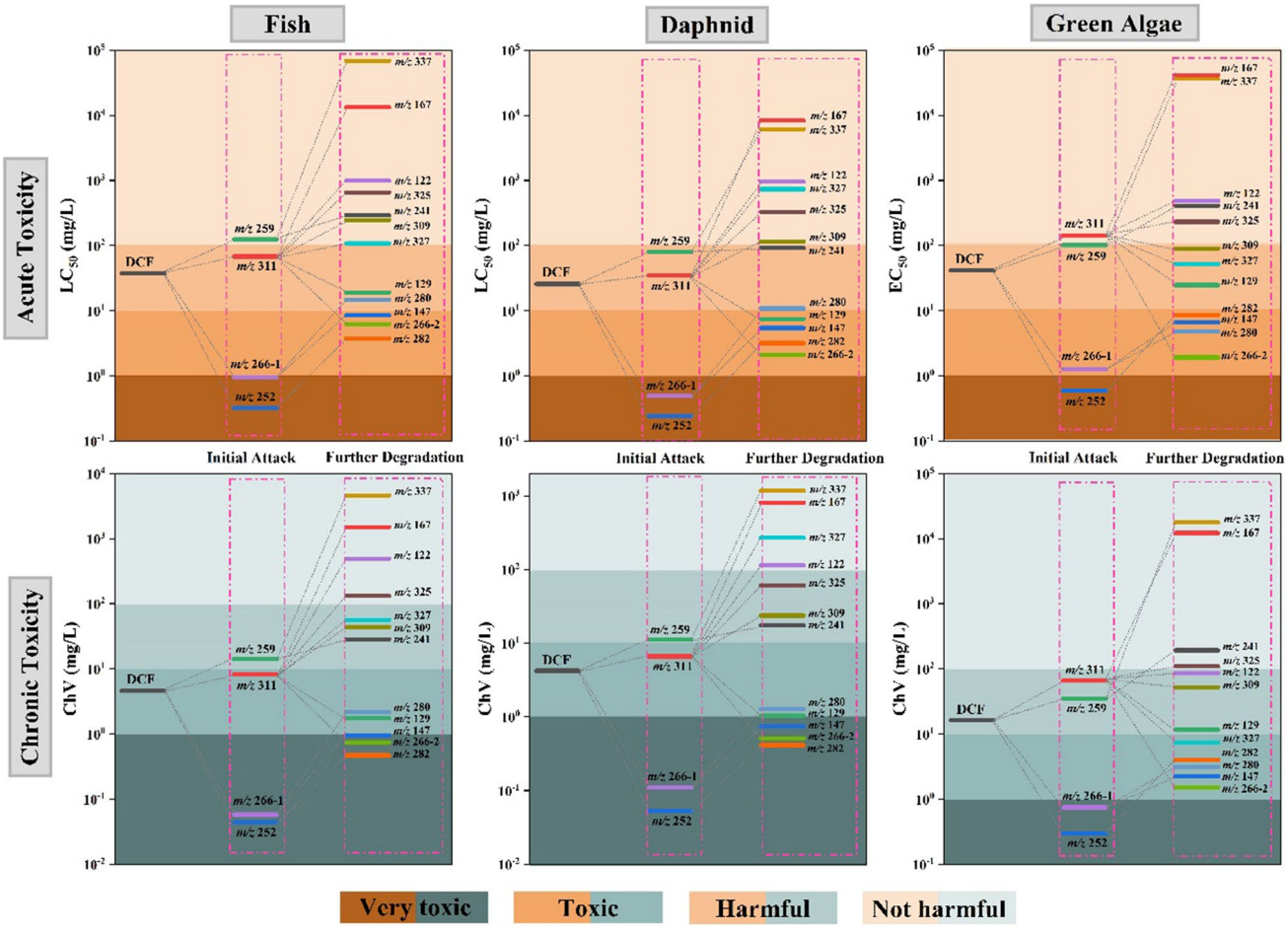

Fig. 11 Toxicity evaluation of DCF and its intermediates in Fe(VI)/PMS system

61.78%, respectively, since the high concentration of TOC and HCO_3^-. The results indicated that the DCF degradation in natural waters by Fe(VI)/PMS could be affected visibly by the water matrix (such as pH, NOM and HCO_3^-).

Conclusions

In this study, the degradation of DCF by Fe(VI)/PMS process was comprehensively explored. Fe(VI)/PMS system can efficiently degrade DCF in aqueous solutions with pH range from 4.0 to 8.0. The removal efficiency of DCF was significantly enhanced with an increase in the reaction temperature (10 to 30 ℃), Fe(VI) dose (6.25 to 100 μM), or PMS concentration (50 to 1000 μM). Inorganic anions NO_3^- and SO_4^{2-} showed almost no effect on DCF oxidation. However, the existences of HCO_3^-, Cl^-, and humic acid (HA) obviously inhibited the removal of DCF. EPR, quenching, and probing experiments revealed that both $SO_4^{\bullet-}$, $^{\bullet}OH$, and Fe(V)/Fe(IV) were responsible for DCF removal in Fe(VI)/PMS system, and the degradation

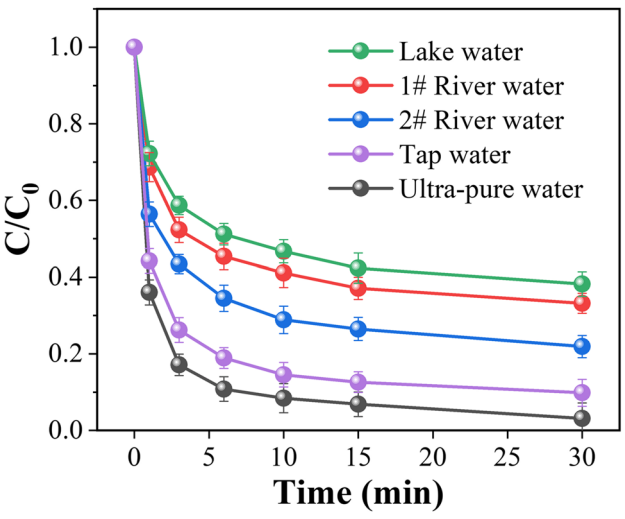

Fig. 12 Degradation of DCF by Fe(VI)/PMS in various types of water. Experimental conditions: $[DCF]_0 = 5$ μM, $[Fe(VI)]_0 = 100$ μM, $[PMS]_0 = 500$ μM, pH = 6, T = 25 ℃

mechanism was evaluated. Compared with the oxidized organics, ferric particles, formed in the reduction of Fe(VI), acted as adsorbent and removed around 30% of TOC in the processes. Hence, the synthetical effect of oxidation and adsorption for DCF removal was revealed in Fe(VI)/PMS system. On the basis of the UPLC-QTOF/MS technique, sixteen DCF degradation byproducts in Fe(VI)/PMS system were detected, and eight reaction pathways were proposed including hydroxylation, decarboxylation, ring closure, dehydrogenation, C-N bond cleavage, formylation, dechlorination-hydroxylation, and sulfonation. Based on the toxicity assessment, some of the intermediates were transformed into developmentally "non harmful," manifesting that the degradation process of DCF by Fe(VI)/PMS was a gradual detoxification process. The DCF removal by Fe(VI)/PMS remained highly efficient in different real waters. This study demonstrates that Fe(VI)/PMS process is an efficient treatment technology for DCF degradation and provides valuable information on the practical application of Fe(VI)/PMS in various aquatic environmental compartments.

Supplementary Information The online version contains supplementary material available at https://doi.org/10.1007/s11356-022-22967-0.

Authors contribution Haonan He: Software, formal analysis, writing-original draft, writing—review and editing, validation.

Junfeng Zhao: Conceptualization, data curation, investigation, supervision, funding acquisition, methodology, resources, project administration.

Funding This work was financially supported by the Startup Project of Scientific Research in Sichuan Normal University (No. 024–341896001) and the Foundation of Key Laboratory of Special Waste Water Treatment, Sichuan Province Higher Education System [SWWT2022-6].

Data availability The datasets used and/or analyzed during the current study are available from the corresponding author on reasonable request.

Declarations

Ethical approval Not applicable.

Consent to participate Not applicable.

Consent to publish Not applicable.

Competing interests The authors declare no competing interests.

References

Agopcan Cinar S, Ziylan-Yavaş A, Catak S, Ince NH, Aviyente V (2017) Hydroxyl radical-mediated degradation of diclofenac revisited: a computational approach to assessment of reaction mechanisms and by-products. Environ Sci Pollut Res 24:18458–18469. https://doi.org/10.1007/s11356-017-9482-7

Al-Abduly A, Sharma VK (2014) Oxidation of benzothiophene, dibenzothiophene, and methyl-dibenzothiophene by ferrate(VI). J Hazard Mater 279:296–301. https://doi.org/10.1016/j.jhazmat.2014.06.083

Anipsitakis GP, Dionysiou DD (2004) Radical generation by the interaction of transition metals with common oxidants. Environ Sci Technol 38:3705–3712. https://doi.org/10.1021/es035121o

Berruti I, Polo-López MI, Oller I, Flores J, Marin ML, Bosca F (2022) Sulfate radical anion: laser flash photolysis study and application in water disinfection and decontamination. Appl Catal B 315:121519. https://doi.org/10.1016/j.apcatb.2022.121519

Bielski BH (1990) Generation of iron(IV) and iron(V) complexes in aqueous solutions. Methods Enzymol 186:108–113. https://doi.org/10.1016/0076-6879(90)86096-E

Bu Q, Wang B, Huang J, Deng S, Yu G (2013) Pharmaceuticals and personal care products in the aquatic environment in China: a review. J Hazard Mater 262:189–211. https://doi.org/10.1016/j.jhazmat.2013.08.040

Cao Y, Qiu W, Li J, Zhao Y, Jiang J, S. Pang S, (2021) Sulfite enhanced transformation of iopamidol by UV photolysis in the presence of oxygen: role of oxysulfur radicals. Water Res 189:116625. https://doi.org/10.1016/j.watres.2020.116625

Chan KH, Chu W (2009) Degradation of atrazine by cobalt-mediated activation of peroxymonosulfate: different cobalt counteranions in homogenous process and cobalt oxide catalysts in photolytic heterogeneous process. Water Res 43:2513–2521. https://doi.org/10.1016/j.watres.2009.02.029

Chen J, Xu X, Zeng X, Feng M, Qu R, Wang Z, Nesnas N, Sharma VK (2018) Ferrate (VI) oxidation of polychlorinated diphenyl sulfides: kinetics, degradation, and oxidized products. Water Res 143:1–9. https://doi.org/10.1016/j.watres.2018.06.023

Chen K, Cui Z, Zhang Z, Pang H, Yang J, Huang X, Lu J (2022a) Life-sustaining of H^+ in S(IV)/Fe(VI) system for efficient removal of dimethoate in water: active species identification and mechanism. Chem Eng J 445:136865. https://doi.org/10.1016/j.cej.2022.136865

Chen Y, Shao Y, Li O, Liang J, Tang S, Li Z (2022b) WS_2-cocatalyzed peroxymonosulfate activation via an enhanced Fe(III)/Fe(II) cycle toward efficient organic pollutant degradation. Chem Eng J 442(1):135961. https://doi.org/10.1016/j.cej.2022.135961

Cheng X, Liang H, Ding A, Tang X, Liu B, Zhu X, Gan Z, Wu D, Li G (2017) Ferrous iron/peroxymonosulfate oxidation as a pretreatment for ceramic ultrafiltration membrane: control of natural organic matter fouling and degradation of atrazine. Water Res 113:32–41. https://doi.org/10.1016/j.watres.2017.01.055

Chi N, Liu J, Feng L, Guo Z, Chen Y, Pan T, Zheng H (2022) FeS redox power motor for PDS continuous generation of active radicals on efficient degradation and removal of diclofenac: role of ultrasonic. Chemosphere 134574. https://doi.org/10.1016/j.chemosphere2022.134574

Chong S, Zhang G, Zhang N, Liu Y, Huang T, Chang H (2017) Diclofenac degradation in water by $FeCeO_x$ catalyzed H_2O_2: influencing factors, mechanism and pathways. J Hazard Mater 334:150–159. https://doi.org/10.1016/j.jhazmat.2017.04.008

Coelho AD, Sans C, Agüera A, Gomez M, Esplugas S, Dezotti M (2009) Effects of ozone pre-treatment on diclofenac: intermediates, biodegradability and toxicity assessment. Sci Total Environ 407:3572–3578. https://doi.org/10.1016/j.scitotenv.2009.01.013

Delaude L, Laszlo P (1996) A novel oxidizing reagent based on potassium ferrate (VI). J Org Chem 61:6360–6370. https://doi.org/10.1021/jo960633p

Ding Y, Pan C, Peng X, Mao Q, Xiao Y, Fu L, Huang J (2020) Deep mineralization of bisphenol A by catalytic peroxymonosulfate activation with nano CuO/Fe_3O_4 with strong Cu-Fe interaction.

Chem Eng J 384:123378. https://doi.org/10.1016/j.cej.2019.123378
Eibenberger H, Steenken S, O'Neill P, Schulte-Frohlinde D (1978) Pulse radiolysis and electron spin resonance studies concerning the reaction of SO2- 4 with alcohols and ethers in aqueous solution. J Phys Chem C 82:749–750. https://doi.org/10.1021/j100495a028
Fei Y, Liu Z, Meng L, Liu G, Kong D, Pan X, Zhu F, Lu J, Chen J (2022) Experimental and theoretical study on Fe(VI) oxidative degradation of dichlorophen in water: kinetics and reaction mechanisms. Environ Pollut 306:119394. https://doi.org/10.1016/j.envpol.2022.119394
Feng MB, Cizmas L, Wang ZY, Sharma VK (2017) Synergistic effect of aqueous removal of fluoroquinolones by a combined use of peroxymonosulfate and ferrate (VI). Chemosphere 177:144–148. https://doi.org/10.1016/j.chemosphere.2017.03.008
Gao Y-Q, Rao Y-Y, Ning H, Chen J-X, Zeng Q, Tian F-X, Gao N-Y (2022) Comparative investigation of diclofenac degradation by Fe^{2+}/chlorine and Fe^{2+}/PMS processes. Sep Purif Technol 297:121555. https://doi.org/10.1016/j.seppur.2022.121555
Gara PMD, Bosio GN, Gonzalez MC, Russo N, Michelini MC, Diez RP, Martire DO (2009) A combined theoretical and experimental study on the oxidation of fulvic acid by the sulfate radical anion. Photochem Photobiol Sci 8:992–997. https://doi.org/10.1039/b900961b
Ghanbari F, Moradi M (2017) Application of peroxymonosulfate and its activation methods for degradation of environmental organic pollutants: review. Chem Eng J 310:41–62. https://doi.org/10.1016/j.cej.2016.10.064
Graham N, Jiang C, Li X-Z, Jiang J-Q, Ma J (2004) The influence of pH on the degradation of phenol and chlorophenols by potassium ferrate. Chemosphere 56:949–956. https://doi.org/10.1016/j.chemosphere.2004.04.060
Hu L, Zhang G, Liu M, Wang Q, Wang P (2018) Enhanced degradation of Bisphenol A (BPA) by peroxymonosulfate with Co_3O_4-Bi_2O_3 catalyst activation: effects of pH, inorganic anions, and water matrix. Chem Eng J 338:300–310. https://doi.org/10.1016/j.cej.2018.01.016
Huang Z-S, Wang L, Liu Y-L, Jiang J, Xue M, Xu C-B, Zhen Y-F, Wang Y-C, Jun Ma J (2018) Impact of phosphate on ferrate oxidation of organic compounds: an underestimated oxidant. Environ Sci Technol 52:13897–13907. https://doi.org/10.1021/acs.est.8b04655
Huang Y, Kong M, Coffin S, Cochran KH, Westerman DC, Schlenk D, Richardson SD, Lei L, Dionysiou DD (2020) Degradation of contaminants of emerging concern by UV/H_2O_2 for water reuse: kinetics, mechanisms, and cytotoxicity analysis. Water Res 174:115587. https://doi.org/10.1016/j.watres.2020.115587
Huang Z-S, Wang L, Liu Y-L, Zhang H-Y, Zhao X-N, Bai Y, Ma J (2021) Ferrate self- decomposition in water is also a self-activation process: role of Fe(V) species and enhancement with Fe(III) in methyl phenyl sulfoxide oxidation by excess ferrate. Water Res 197:117094. https://doi.org/10.1016/j.watres.2021.117094
Huguet M, Deborde M, Papot S, Gallard H (2013) Oxidative decarboxylation of diclofenac by manganese oxide bed filter. Water Res 47(14):5400–5408. https://doi.org/10.1016/j.watres.2013.06.016
Jiang J-Q (2014) Advances in the development and application of ferrate(VI) for water and wastewater treatment. J Chem Technol Biotechnol 89:165–177. https://doi.org/10.1002/jctb.4214
Jiang J-Q, Stanford C, Alsheyab M (2009) The online generation and application of ferrate (VI) for sewage treatment—A pilot scale trial. Sep Purif Technol 68:227–231. https://doi.org/10.1016/j.seppur.2009.05.007
Jiang Y, Goodwill JE, Tobiason JE, Reckhow DA (2015) Effect of different solutes, natural organic matter, and particulate Fe (III) on ferrate (VI) decomposition in aqueous solutions. Environ Sci Technol 49:2841–2848. https://doi.org/10.1021/es505516w
Jiang Y, Goodwill JE, Tobiason JE, Reckhow DA (2016) Impacts of ferrate oxidation on natural organic matter and disinfection byproduct precursors. Water Res 96:114–125. https://doi.org/10.1016/j.watres.2016.03.052
Jin Q, Ji D, Chen Y, Tang Z, Fu Y (2022) Kinetics and pathway of levofloxacin degradation by ferrate(VI) and reaction mechanism of catalytic degradation by copper sulfide. Sep Purif Technol 282 B:120104. https://doi.org/10.1016/j.seppur.2021.120104
Joss A, Keller E, Alder AC, Gobel A, McArdell CS, Ternes T, Siegrist H (2005) Removal of pharmaceuticals and fragrances in biological wastewater treatment. Water Res 39:3139–3152. https://doi.org/10.1016/j.watres.2005.05.031
Khan JA, He X, Shah NS, Khan HM, Hapeshi E, Fatta-Kassinos D, Dionysiou DD (2014) Kinetic and mechanism investigation on the photochemical degradation of atrazine with activated H_2O_2, S_2O2- 8 and HSO− 5. Chem Eng J 252:393–403. https://doi.org/10.1016/j.cej.2014.04.104
Kong XJ, Jiang J, Ma J, Yang Y, Pang SY (2018) Comparative investigation of X-ray contrast medium degradation by UV/chlorine and UV/H_2O_2. Chemosphere 193:655–663. https://doi.org/10.1016/j.chemosphere.2017.11.064
Lan BY, Wang YX, Wang X, Zhou XT, Kang Y, Li LS (2016) Aqueous arsenic (As) and antimony (Sb) removal by potassium ferrate. Chem Eng J 292:389–397. https://doi.org/10.1016/j.cej.2016.02.019
Lee Y, Yoon J, von Gunten U (2005) Kinetics of the Oxidation of Phenols and Phenolic Endocrine Disruptors during Water Treatment with Ferrate (Fe(VI)). Environ Sci Technol 39:8978–8984. https://doi.org/10.1021/es051198w
Lee Y, Kissner R, von Gunten U (2014) Reaction of ferrate (VI) with ABTS and self-decay of ferrate (VI): kinetics and mechanisms. Environ Sci Technol 48:5154–5162. https://doi.org/10.1021/es500804g
Li X, Liu X, Lin C, Zhou Z, He M, Ouyang W (2020) Catalytic oxidation of contaminants by Fe^0 activated peroxymonosulfate process: Fe(IV) involvement, degradation intermediates and toxicity evaluation. Chem Eng J 382:123013. https://doi.org/10.1016/j.cej.2019.123013
Liang C, Huang C-F, Mohanty N, Kurakalva RM (2008) A rapid spectrophotometric determination of persulfate anion in ISCO. Chemosphere 73:1540–1543. https://doi.org/10.1016/j.chemosphere.2008.08.043
Liu S, Zhao X, Zeng H, Wang Y, Qiao M, Guan W (2017a) Enhancement of photoelectrocatalytic degradation of diclofenac with persulfate activated by Cu cathode. Chem Eng J 320:168–177. https://doi.org/10.1016/j.cej.2017.03.047
Liu Y-L, Wang L, Wang X, Huang Z, Xu C, Yang T, Zhao X, Qi J, Ma J (2017b) Highly efficient removal of trace Thallium from contaminated source waters with ferrate: role of *in situ* formed ferric nanoparticle. Water Res 124:149–157. https://doi.org/10.1016/j.watres.2017.07.051
Liu YD, Zhou AG, Gan YQ, Li XQ (2018) Roles of hydroxyl and sulfate radicals in degradation of trichloroethene by persulfate activated with Fe^{2+} and zero-valent iron: insights from carbon isotope fractionation. J Hazard Mater 344:98–103. https://doi.org/10.1016/j.jhazmat.2017.09.048
Liu H, Chen J, Wu N, Xu X, Qi Y, Jiang L, Wang X, Wang Z (2019) Oxidative degradation of chlorpyrifos using ferrate (VI): kinetics and reaction mechanism. Ecotoxicol Environ Saf 170:259–266. https://doi.org/10.1016/j.ecoenv.2018.11.132
Luo R, Liu C, Li J, Wang J, Hu X, Sun X, Shen J, Han W, Wang L (2017) Nanostructured CoP: an efficient catalyst for degradation of organic pollutants by activating peroxymonosulfate. J

Hazard Mater 329:92–101. https://doi.org/10.1016/j.jhazmat.2017.01.032
Luo C, Feng M, Sharma VK, Huang C-H (2019) Oxidation of pharmaceuticals by ferrate(VI) in hydrolyzed urine: effects of major inorganic constituents. Environ Sci Technol 53(9):5272–5281. https://doi.org/10.1021/acs.est.9b00006
Mahdi-Ahmed M, Chiron S (2014) Ciprofloxacin oxidation by UV-C activated peroxymonosulfate in wastewater. J Hazard Mater 265:41–46. https://doi.org/10.1016/j.jhazmat.2013.11.034
Manoli K, Maffettone R, Sharma VK (2020) Inactivation of Murine Norovirus and Fecal Coliforms by Ferrate(VI) in Secondary Effluent Wastewater. Environ Sci Technol 54:1878–1888. https://doi.org/10.1021/acs.est.9b05489
Martínez C, Fernández MI, Santaballa JA, Faria J (2011) Aqueous degradation of diclofenac by heterogeneous photocatalysis using nanostructured materials. Appl Catal B 107:110–118. https://doi.org/10.1016/j.apcatb.2011.07.003
Melton JD, Bielski BH (1990) Studies of the kinetic spectral and chemical properties of Fe(IV) pyrophosphate by pulse radiolysis. Radiat Phys Chem 36(6):725–733.https://doi.org/10.1016/1359-0197(90)90169-I
Monteagudo JM, El-taliawy H, Durán A, Caro G, Bester K (2018) Sono-activated persulfate oxidation of diclofenac: degradation, kinetics, pathway and contribution of the different radicals involved. J Hazard Mater 357:457–465. https://doi.org/10.1016/j.jhazmat.2018.06.031
Nie M, Yan C, Xiong X, Wen X, Yang X, Lv Z, Dong W (2018) Degradation of chloramphenicol using a combination system of simulated solar light, Fe^{2+} and persulfate. Chem Eng J 348:455–463. https://doi.org/10.1016/j.cej.2018.04.124
Oh W-D, Dong Z, Lim T-T (2016) Generation of sulfate radical through heterogeneous catalysis for organic contaminants removal: current development, challenges and prospects. Appl Catal B 194:169–201. https://doi.org/10.1016/j.apcatb.2016.04.003
Oleg P, Andreja B (2004) Reactivity of Aqueous Fe(IV) in Hydride and Hydrogen Atom Transfer Reactions. J Am Chem Soc 126:13757–13764. https://doi.org/10.1021/ja0457112
Olmez-Hanci T, Arslan-Alaton I (2013) Comparison of sulfate and hydroxyl radical based advanced oxidation of phenol. Chem Eng J 224:10–16. https://doi.org/10.1016/j.cej.2012.11.007
Oral O, Kantar C (2019) Diclofenac removal by pyrite-Fenton process: performance in batch and fixed-bed continuous flow systems. Sci Total Environ 664:817–823. https://doi.org/10.1016/j.scitotenv.2019.02.084
Petrie B, Barden R, Kasprzyk-Hordern B (2015) A review on emerging contaminants in wastewaters and the environment: current knowledge, understudied areas and recommendations for future monitoring. Water Res 72:3–27. https://doi.org/10.1016/j.watres.2014.08.053
Rao YF, Zhang YF, Han FM, Guo HC, Huang Y, Li RY, Qi F, Ma J (2018) Heterogeneous activation of peroxymonosulfate by $LaFeO_3$ for diclofenac degradation: DFT-assisted mechanistic study and degradation pathways. Chem Eng J 352:601–611. https://doi.org/10.1016/j.cej.2018.07.062
Salaeh S, Perisic DJ, Biosic M, Kusic H, Babic S, Stangar UL, Dionysiou DD, Bozic AL (2016) Diclofenac removal by simulated solar assisted photocatalysis using TiO_2-based zeolite catalyst; mechanisms, pathways and environmental aspects. Chem Eng J 304:289–302. https://doi.org/10.1016/j.cej.2016.06.083
Shao B, Dong H, Bo Sun B, Guan X (2019) Role of Ferrate(IV) and Ferrate(V) in Activating Ferrate(VI) by Calcium Sulfite for Enhanced Oxidation of Organic Contaminants. Environ Sci Technol 53(2):894–902. https://doi.org/10.1021/acs.est.8b04990
Shao B, Dong H, Feng L, Qiao J, Guan X (2020) Influence of [sulfite]/[Fe(VI)] molar ratio on the active oxidants generation in Fe(VI)/sulfite process. J Hazard Mater 384:121303. https://doi.org/10.1016/j.jhazmat.2019.121303
Sharma VK (2002) Potassium ferrate (VI): an environmentally friendly oxidant. Adv Environ Res 6:143–156. https://doi.org/10.1016/S1093-0191(01)00119-8
Sharma VK (2008) Oxidative transformations of environmental pharmaceuticals by Cl_2, ClO_2, O_3, and Fe(VI): kinetics assessment. Chemosphere 73(9):1379–1386. https://doi.org/10.1016/j.chemosphere.2008.08.033
Sharma VK (2010) Oxidation of nitrogen-containing pollutants by novel ferrate (VI) technology: a review. J Environ Sci Health A 45:645–667. https://doi.org/10.1080/10934521003648784
Sharma VK (2011) Oxidation of inorganic contaminants by ferrates (VI, V, and IV)–kinetics and mechanisms: a review. J Environ Manage 92(4):1051–1073. https://doi.org/10.1016/j.jenvman.2010.11.026
Sharma VK (2013) Ferrate (VI) and ferrate (V) oxidation of organic compounds: kinetics and mechanism. Coord Chem Rev 257:495–510. https://doi.org/10.1016/j.ccr.2012.04.014
Sharma J, Mishra IM, Dionysiou DD, Kumar V (2015a) Oxidative removal of Bisphenol A by UV-C/peroxymonosulfate (PMS): kinetics, influence of co-existing chemicals and degradation pathway. Chem Eng J 276:193–204. https://doi.org/10.1016/j.cej.2015.04.021
Sharma J, Mishra IM, Kumar V (2015b) Degradation and mineralization of Bisphenol A (BPA) in aqueous solution using advanced oxidation processes: UV/H_2O_2 and UV/S2O2- 8oxidation systems. J Environ Manage 156:266–275. https://doi.org/10.1016/j.jenvman.2015.03.048
Sharma VK, Zboril R, Varma RS (2015c) Ferrates: greener oxidants with multimodal action in water treatment technologies. Acc Chem Res 48:182–191. https://doi.org/10.1021/ar5004219
Sharma VK, Feng M, Dionysiou DD, Zhou H-C, Jinadatha C, Manoli K, Smith MF, Luque R, Ma X, Huang C-H (2022) Reactive high-valent iron intermediates in enhancing treatment of water by ferrate. Environ Sci Technol 56:30–47. https://doi.org/10.1021/acs.est.1c04616
Sheikhi S, Jebalbarezi B, Dehghanzadeh R, Maryamabadi A, Aslani H (2022) Sulfamethoxazole oxidation in secondary treated effluent using Fe(VI)/PMS and Fe(VI)/H_2O_2 processes: experimental parameters, transformation products, reaction pathways and toxicity evaluation. J Environ Chem Eng 10(3):107446. https://doi.org/10.1016/j.jece.2022.107446
Shi Z, Wang D, Gao Z, Ji X, Zhang J, Jin C (2022) Enhanced ferrate oxidation of organic pollutants in the presence of Cu(II) Ion. J Hazard Mater 433:128772. https://doi.org/10.1016/j.jhazmat.2022.128772
Simonsen LO, Harbak H, Bennekou P (2012) Cobalt metabolism and toxicology—A brief update. Sci Total Environ 432:210–215. https://doi.org/10.1016/j.scitotenv.2012.06.009
Sun X, Feng M, Dong S, Qi Y, Sun L, Nesnas N, Sharma VK (2019) Removal of sulfachloropyridazine by ferrate(VI): kinetics, reaction pathways, biodegradation, and toxicity evaluation. Chem Eng J 372:742–751. https://doi.org/10.1016/j.cej.2019.04.121
Tian S-Q, Wang L, Liu Y-L, Ma J (2020) Degradation of organic pollutants by ferrate/biochar: enhanced formation of strong intermediate oxidative iron species. Water Res 183:116054. https://doi.org/10.1016/j.watres.2020.116054
Waclawek S, Lutze HV, Grübel K, Padil VVT, Cernik M, Dionysiou DD (2017) Chemistry of persulfates in water and wastewater treatment: a review. Chem Eng J 330:44–62. https://doi.org/10.1016/j.cej.2017.07.132

Wang J, Bai Z (2017) Fe-based catalysts for heterogeneous catalytic ozonation of emerging contaminants in water and wastewater. Chem Eng J 312:79–98. https://doi.org/10.1016/j.cej.2016.11.118

Wang J, Wang S (2018) Activation of persulfate (PS) and peroxymonosulfate (PMS) and application for the degradation of emerging contaminants. Chem Eng J 334:1502–1517. https://doi.org/10.1016/j.cej.2017.11.059

Wang P, Yang S, Shan L, Niu R, Shao X (2011) Involvements of chloride ion in decolorization of Acid Orange 7 by activated peroxydisulfate or peroxymonosulfate oxidation. J Environ Sci 23:1799–1807. https://doi.org/10.1016/S1001-0742(10)60620-1

Wang Y, Liu H, Liu G, Xie Y (2014) Oxidation of diclofenac by aqueous chlorine dioxide: identification of major disinfection byproducts and toxicity evaluation. Sci Total Environ 473:437–445. https://doi.org/10.1016/j.scitotenv.2013.12.056

Wang S, Xu W, Wu J, Gong Q, Xie P (2020) Improved sulfamethoxazole degradation by the addition of MoS_2 into the Fe^{2+}/peroxymonosulfate process. Sep Purif Technol 235:116170. https://doi.org/10.1016/j.seppur.2019.116170

Wang H, Deng J, Lu X, Wan L, Huang J, Liu Y (2021) Rapid and continuous degradation of diclofenac by Fe(II)-activated persulfate combined with bisulfite. Sep Purif Technol 262:118335. https://doi.org/10.1016/j.seppur.2021.118335

Wang Z, Wang F, Xiang L, Bian Y, Zhao Z, Gao Z, Cheng J, Schaeffer A, Jiang X, Dionysiou DD (2022) Degradation of mineral-immobilized pyrene by ferrate oxidation: role of mineral type and intermediate oxidative iron species. Water Res 217:118377. https://doi.org/10.1016/j.watres.2022.118377

Wei Z, Villamena FA, Weavers LK (2017) Kinetics and mechanism of ultrasonic activation of persulfate: an in situ EPR spin trapping study. Environ Sci Technol 51:3410–3417. https://doi.org/10.1021/acs.est.6b05392

Wu MH, Shi J, Deng HP (2018a) Metal doped manganese oxide octahedral molecular sieve catalysts for degradation of diclofenac in the presence of peroxymonosulfate. Arab J Chem 11:924–934. https://doi.org/10.1016/j.arabjc.2018.02.002

Wu S, Li H, Li X, He H, Yang C (2018b) Performances and mechanisms of efficient degradation of atrazine using peroxymonosulfate and ferrate as oxidants. Chem Eng J 353:533–541. https://doi.org/10.1016/j.cej.2018.06.133

Wu Y, Yang Y, Liu Y, Zhang L, Feng L (2019) Modelling study on the effects of chloride on the degradation of bezafibrate and carbamazepine in sulfate radical-based advanced oxidation processes: conversion of reactive radicals. Chem Eng J 358:1332–1341. https://doi.org/10.1016/j.cej.2018.10.125

Xiao R, Luo Z, Wei Z, Luo S, Spinney R, Yang W, Dionysiou DD (2018) Activation of peroxymonosulfate/persulfate by nanomaterials for sulfate radical-based advanced oxidation technologies. Curr Opin Chem Eng 19:51–58. https://doi.org/10.1016/j.coche.2017.12.005

Xiao S, Cheng M, Zhong H, Liu Z, Liu Y, Yang X, Liang Q (2020) Iron-mediated activation of persulfate and peroxymonosulfate in both homogeneous and heterogeneous ways: a review. Chem Eng J 384:123265. https://doi.org/10.1016/j.cej.2019.123265

Xu GR, Zhang YP, Li GB (2009) Degradation of azo dye active brilliant red X-3B by composite ferrate solution. J Hazard Mater 161(2–3):1299–1305. https://doi.org/10.1016/j.jhazmat.2008.04.090

Xu P, Xie S, Liu X, Wang L, Jia X, Yang C (2022) Electrochemical enhanced heterogenous activation of peroxymonosulfate using $CuFe_2O_4$ particle electrodes for the degradation of diclofenac. Chem Eng J 446(1):136941. https://doi.org/10.1016/j.cej.2022.136941

Yang B, Ying G-G, Zhao J-L, Liu S, Zhou L-J, Chen F (2012) Removal of selected endocrine disrupting chemicals (EDCs) and pharmaceuticals and personal care products (PPCPs) during ferrate(VI) treatment of secondary wastewater effluents. Water Res 46:2194–2204. https://doi.org/10.1016/j.watres.2012.01.047

Yang Y, Pignatello JJ, Ma J, Mitch WA (2014) Comparison of halide impacts on the efficiency of contaminant degradation by sulfate and hydroxyl radical-based advanced oxidation processes (AOPs). Environ Sci Technol 48:2344–2351. https://doi.org/10.1021/es404118q

Yang T, Liu Y, Wang L, Jiang J, Huang Z, Pang S-Y, Cheng H, Gao D, Ma J (2018) Highly effective oxidation of roxarsone by ferrate and simultaneous arsenic removal with *in situ* formed ferric nanoparticles. Water Res 147:321–330. https://doi.org/10.1016/j.watres.2018a.10.012

Yang T, Wang L, Liu Y-L, Jiang J, Huang Z, Pang S, Cheng H, Gao D, Ma J (2018) Removal of organoarsenic with ferrate and ferrate resultant nanoparticles: oxidation and adsorption. Environ Sci Technol 52:13325–13335. https://doi.org/10.1021/acs.est.8b01718

Yang T, Wang L, Liu Y, Huang Z, He H, Wang X, Jiang J, Gao D, Ma J (2019) Comparative study on ferrate oxidation of BPS and BPAF: kinetics, reaction mechanism, and the improvement on their biodegradability. Water Res 148:115–125. https://doi.org/10.1016/j.watres.2018.10.018

Yang T, Wu S, Mai J, Chen L, Huang C, Zeng G, Wu Y, Zhu M, Huang Y, Mo Z, Guo L, Jia J, Ma J (2022) Activation of ferrate(VI) by sulfite for effectively degrading iodinated contrast media and synchronously controlling I-DBPs formation. Chem Eng J 442:136011. https://doi.org/10.1016/j.cej.2022.136011

Yu J, Jiao R, Sun H, Xu H, He Y, Wang D (2022) Removal of microorganic pollutants in aquatic environment: the utilization of Fe(VI). J Environ Manage 316:115328. https://doi.org/10.1016/j.jenvman.2022.115328

Zhang J, Zhao W, Wu S, Yin R, Zhu M (2021) Surface dual redox cycles of Mn(III)/Mn(IV) and Cu(I)/Cu(II) for heterogeneous peroxymonosulfate activation to degrade diclofenac: performance, mechanism and toxicity assessment. J Hazard Mater 410:124623. https://doi.org/10.1016/j.jhazmat.2020.124623

Zhang J, Chen Y, Song X, Liu Y, Zhao J, Wang F (2022) Synergistic adsorption and degradation of diclofenac by zero-valent iron modified spent bleaching earth carbon: mechanism and toxicity assessment. J Hazard Mater 128753. https://doi.org/10.1016/j.jhazmat.2022.128753

Zhao J, Liu Y, Wang Q, Fu Y, Lu X, Bai X (2018a) The self-catalysis of ferrate (VI) by its reactive byproducts or reductive substances for the degradation of diclofenac: kinetics, mechanism and transformation products. Sep Purif Technol 192:412–418. https://doi.org/10.1016/j.seppur.2017.10.030

Zhao J, Wang Q, Fu Y, Peng B, Zhou G (2018b) Kinetics and mechanism of diclofenac removal using ferrate (VI): roles of Fe^{3+}, Fe^{2+}, and Mn^{2+}. Environ Sci Pollut Res 25:22998–23008. https://doi.org/10.1007/s11356-018-2375-6

Zhang M, Chen X, Zhou H, Murugananthan M, Zhang Y (2015) Degradation of p-nitrophenol by heat and metal ions co-activated persulfate. Chem Eng J 264:39–47. https://doi.org/10.1016/j.cej.2014.11.060

Zhao W, Duan Z, Zheng Z, Li B (2022) Efficient diclofenac removal by superoxide radical and singlet oxygen generated in surface Mn (II)/(III)/(IV) cycle dominated peroxymonosulfate activation system: mechanism and product toxicity. Chem Eng J 433:133742. https://doi.org/10.1016/j.cej.2021.133742

Zhao W, Duan Z, Zheng Z, Li B (2022b) Cobalt bismuth oxide with cobalt(II/III) as a new stable peroxymonosulfate activator for effective degradation, mineralization, and detoxification of

diclofenac in water. J Clean Prod 365:132781. https://doi.org/10.1016/j.jclepro.2022.132781

Zhen G, Lu X, Su L, Kobayashi T, Kumar G, Zhou T, Xu K, Li Y-Y, Zhu X, Zhao Y (2018) Unraveling the catalyzing behaviors of different iron species (Fe^{2+} vs. Fe^{0}) in activating persulfate-based oxidation process with implications to waste activated sludge dewaterability. Water Res 134:101–114. https://doi.org/10.1016/j.watres.2018.01.072

Zhen G, Lu X, Zhao Y, Chai X, Niu D (2012) Enhanced dewaterability of sewage sludge in the presence of Fe (II)-activated persulfate oxidation. Bioresour Technol 116:259–265. https://doi.org/10.1016/j.biortech.2012.01.170

Zhou Z, Jiang J-Q (2015) Treatment of selected pharmaceuticals by ferrate (VI): performance, kinetic studies and identification of oxidation products. J Pharm Biomed Anal 106:37–45. https://doi.org/10.1016/j.jpba.2014.06.032

Zhu J, Yu F, Meng J, Shao B, Dong H, Chu W, Cao T, Wei G, Wang H, Guan X (2020) Overlooked role of Fe(IV) and Fe(V) in organic contaminant oxidation by Fe(VI). Environ Sci Technol 54:9702–9710. https://doi.org/10.1021/acs.est.0c03212

Zuo Z, Cai Z, Katsumura Y, Chitose N, Muroya Y (1999) Reinvestigation of the acid–base equilibrium of the (bi) carbonate radical and pH dependence of its reactivity with inorganic reactants. Radiat Phys Chem 55:15–23. https://doi.org/10.1016/S0969-806X(98)00308-9